HHS Public Access

Author manuscript

J Med Chem. Author manuscript; available in PMC 2016 July 23.

Published in final edited form as:

J Med Chem. 2015 July 23; 58(14): 5459–5475. doi:10.1021/acs.jmedchem.5b00391.

Synthesis and Pharmacokinetic Evaluation of Siderophore Biosynthesis Inhibitors for *Mycobacterium tuberculosis*

Kathryn M. Nelson[a,#], **Kishore Viswanathan**[b,#], **Surendra Dawadi**[b], **Benjamin P. Duckworth**[a], **Helena I. Boshoff**[c], **Clifton E. Barry 3rd**[c], and **Courtney C. Aldrich**[a,b,*]

[a]Center for Drug Design, Academic Health Center, University of Minnesota, Minneapolis, MN 55455, USA

[b]Department of Medicinal Chemistry, University of Minnesota, Minneapolis, Minnesota, MN 55455, USA

[c]Tuberculosis Research Section, National Institute of Allergy and Infectious Diseases, Bethesda, MD 20892, USA

Abstract

MbtA catalyzes the first committed biosynthetic step of the mycobactins, which are important virulence factors associated with iron acquisition in *Mycobacterium tuberculosis*. MbtA is a validated therapeutic target for antitubercular drug development. 5′-*O*-[*N*-(salicyl)sulfamoyl]adenosine (**1**) is a bisubstrate inhibitor of MbtA and exhibits exceptionally potent biochemical and antitubercular activity. However, **1** suffers from sub-optimal drug disposition properties resulting in a short half-life ($t_{1/2}$), low exposure (AUC), and low bioavailability (F). Four strategies were pursued to address these liabilities including the synthesis of prodrugs, increasing the pK_a of the acyl-sulfonyl moiety, modulation of the lipophilicity, and strategic introduction of fluorine into **1**. Complete pharmacokinetic (PK) analysis of all compounds was performed. The most successful modifications involved fluorination of the nucleoside that provided substantial improvements in $t_{1/2}$ and AUC. Increasing the pK_a of the acyl-sulfonyl linker yielded incremental enhancements while modulation of the lipophilicity and prodrug approaches led to substantially poorer PK parameters.

Introduction

Mycobacterium tuberculosis (*Mtb*), often considered the most successful human pathogen, infects more than two billion people and remains a leading source of infectious disease mortality and morbidity.[1] Tuberculosis (TB), the disease caused by *Mtb* or one of seven other closely related *Mycobacterium* species,[2] has received renewed attention since the

Corresponding Author Footnote: To whom correspondence should be addressed. Phone 612-625-7956. Fax 612-626-3114. aldri015@umn.edu.

[#]**Author Contributions:** These authors contributed equally

Supporting Information: Copies of ^{1}H NMR and ^{13}C NMR spectra of all new compounds, concentration-response curves of **5–10** with MbtA, mean plasma concentration *vs*. time curves of oral and intravenous doses for **1, 4–10**, and serum stability studies of **3**. This material is available free of charge via the Internet at http://pubs.acs.org.

Notes: The authors declare no competing financial interests.

World Health Organization (WHO) declared TB a global health emergency due the alarming rise of drug resistance, pandemic of HIV-TB co-infection, and lack of new therapeutics.[1] Multidrug resistant TB (MDR-TB) is defined as resistance to isoniazid and rifampin, which are the two most effective TB drugs. Approximately, 9% of MDR-TB cases are additionally resistant to one of the injectable antibiotics used for TB (aminoglycosides or capreomycins) and any fluoroquinoline; these TB strains are classified as extensively drug resistant (XDR-TB).[1] *Mtb* is extraordinarily difficult to treat, requiring prolonged therapy with multiple antibiotics for 6 months for simple drug susceptible infections[3] and up to 20 months for drug-resistant infections, with poor treatment outcomes in the latter cases.[4] Eradication of the global TB pandemic, a long-term goal of the WHO, will require improved diagnostics, vaccines, and new drugs. Excellent progress has been made over the last decade and, for the first time in over forty years, two new TB drugs (Bedaquiline and Delamanid) were approved for MDR-TB by US and European regulatory agencies; although initial enthusiasm has been marred by safety concerns.[5, 6] While a specific target candidate profile has not yet been established in the TB field, ideal criteria for new antitubercular agents as advocated by the TB Alliance (http://www.tballiance.org) include: the potential to shorten and simplify the treatment regimen, effectiveness against multidrug resistant strains, and compatibility with HIV-TB co-infection.

In conceiving of new therapeutic strategies for TB we have focused on mycobacterial iron acquisition, an essential *Mtb* process with a long, storied history. In the mid-19th century, decades before Robert Koch identified *Mtb* as the etiological agent of TB, the famous French physician Armand Trousseau noticed some anemic patients rapidly succumbed to TB reactivation when given iron supplements.[7] This observation is now mechanistically understood since *Mtb*, as well as most microorganisms, requires iron as a redox cofactor for numerous essential cellular processes. However, normal physiological conditions restrict the free ferric concentration to an estimated 10^{-24} M, far below the concentration the bacteria needs for proliferation.[8, 9] The process of withholding an essential nutrient is referred to as nutritional immunity, and represents an extremely effective strategy to prevent bacterial growth. To combat iron deficiency, bacteria produce small molecule iron chelators known as siderophores, often at great metabolic expense, that are secreted into the surrounding environment and abstract iron from host proteins.[10, 11] The siderophore-ferric complexes are then reimported into the bacteria cytosol, usually by specific siderophore transporters, where iron is released through hydrolytic destruction of the siderophore or through reduction of Fe^{3+} to Fe^{2+}. The tripodal mycobactins produced by *Mycobacterium* species were the first class of siderophores characterized in 1912 and found to be an essential substance for mycobacterial growth.[12–14] Siderophores of diverse chemical structures are now known to be produced by virtually all microorganisms, and even some plants.[15, 16]

Following the publication of the *Mtb* genome in 1998, the Walsh group identified a locus of 10 genes (*mbtA-J*) encoding for a mixed nonribosomal peptide synthetase-polyketide synthase (NRPS-PKS) pathway responsible for biosynthesis of the mycobactin peptidic core. This was subsequently verified through comprehensive mutational analysis and functional characterization.[17–19] Gokhale and co-workers later identified a second locus of four genes (*mbtK-N*) required for synthesis of the lipid side-chain found in the

mycobactins.[20] *Mtb* mutants deficient in mycobactin production or transport have been shown to have severe growth defects under iron limiting conditions, and are incapable of establishing an infection in vivo.[21–23] Collectively, these results provide compelling evidence for targeting iron acquisition in *Mtb* with small molecules. Indeed, two diametrically opposed approaches have been pursued through synthesis of mycobactin analogues and inhibitors of mycobactin biosynthesis.[24, 25] In spectacular application of the first approach, Miller and co-workers synthesized a mycobactin-artemisinin conjugate that exploits the mycobactin uptake system for delivery of artemisinin, which generates toxic reactive oxygen species upon intracellular reductive release of Fe^{2+} from mycobactin.[26] Inhibition of mycobactin biosynthesis has also been fruitful, and inhibitors of enzymes within the pathway have been described for MbtA,[25, 27, 28] MbtI,[29] MbtM,[30] and PptT.[31]

MbtA, responsible for incorporation of salicylic acid into the mycobactin core structure, has been the most extensively studied for inhibitor development. [28, 32–36] The bisubstrate inhibitor 5′-*O*-[*N*-(salicyl)sulfamoyl]adenosine (**1**, Figure 1C) was independently described by three groups and found to exhibit exceptionally potent enzyme inhibition of MbtA, with an apparent K_i of ∼6 nM under physiologically relevant super-saturating concentrations of its substrates ATP and salicylic acid.[25, 27, 28] This compound possesses potent antitubercular activity, with a minimum inhibitory concentration of 0.39 μM under iron-limiting conditions *in vitro*, and was also effective in an acute murine TB infection model when dosed intraperitoneally, thereby chemically validating MbtA as an antitubercular target.[37] Unfortunately, **1** possesses sub-optimal pharmacokinetic (PK) parameters including poor oral bioavailability, low oral exposure, and rapid clearance.[37] We report herein four approaches to address the poor PK parameters of **1** including: the synthesis of prodrugs (**2–3**), analogs that increase the sulfamate pK_a (**4–5**), modulation of the lipophiliciy of the highly polar nucleoside (**6–7**), and strategic introduction of fluorine into the nucleoside (**8–10**) as shown in Figure 1C. Pharmacokinetic analysis of all compounds was performed in conjunction with selective *in vitro* studies to understand the PK behavior.

Results and Discussion

Chemistry

The simple di-acetate prodrug **2**, wherein the polar 2′ and 3′ alcohols are masked, as well as tri-acetate **3**, in which the phenol is additionally acylated, were initially explored to improve the bioavailability and exposure of **1**. Acetates are quickly hydrolyzed by serum esterases *in vivo*.[38] The di-acetate **2** was obtained by acylation of sulfamate **11**[39] with *N*-hydroxysuccinimidyl 2-benzyloxybenzoate[28] to provide **12** (Scheme 1A). Trifluoracetic acid (TFA) mediated deprotection of the acetonide followed by acetylation of the resultant free 2′ and 3′ alcohols afforded **13**. Catalytic hydrogenolysis and reverse-phase high performance liquid chromatography (HPLC) purification furnished di-acetate product **2**. The tri-acetate derivative **3** was prepared by direct acetylation of **1** employing acetic anhydride and pyridine in dimethylformamide (DMF) (Scheme 1B). These conditions were notable since competitive acetylation at the N^6 position of adenosine was not observed. Compound **3** was first purified on normal phase silica and isolated as an approximate 5:1 mixture of tri-and di-acetates **3** and **2**. Further purification by reverse-phase HPLC was required to obtain pure **3**.

In an effort to further increase the pK_a of the acylsulfonyl linker's acidic nitrogen, the next analogues in this set replaced the sulfamate linker with a sulfamide and added a *para*-amino substitution on the salicyl moiety to provide **4** and **5**, respectively (Scheme 2). We developed a new synthesis of **4** (i.e. **14**→**15**→**16**→**4**) resulting in a 10-fold improved overall yield relative to our initially disclosed route.[28] Our revised synthesis features a Mitsunobu reaction of *tert*-butoxycarbonyl (Boc) sulfamide (**29**)[40] with N^6,N^6-bis(Boc)-isopropylideneadenosine (**14**)[39] to afford **15** in an impressive 96% yield for direct installation of the sulfamide group at C-5′ of the nucleoside. Here the N^6-bis-Boc protecting group in **14** is essential to subdue cyclonucleoside formation that occurs from cyclization of N-3 onto C-5' during the Mitsunobu reaction by attenuating the nucleophilicity at N-3.[41, 42] Coupling **15** to the *N*-hydroxysuccinimide (NHS) ester of 2-*O*-methoxymethylsalicyate (**31**)[32] employing Cs_2CO_3 in DMF provided **16** in 60% yield. The adjacent Boc group on the sulfamide moiety is responsible for the reduced yields of this acylation reaction relative to that observed with simple sulfamate analogs, which typically proceed in 80–90% yields. Global deprotection with 80% aqueous TFA furnished sulfamide **4** that was purified by reverse-phase HPLC and isolated in 65% yield as the triethylammonium salt. Compound **5** was prepared in an analogous fashion (**15**→**17**→**18**→**5**) except sulfamide **15** was acylated with benzyloxycarbonyl (Cbz) protected *p*-aminosalicylate (**32**)[43] employing in situ activation with carbonyl diimidazole (CDI)[25, 33] to afford **17**. Sequential hydrogenolysis of the Cbz group with Pd/C in methanol to **18** followed by acidic deprotection furnished **5**.

N^6-Cyclopropyl **6** and N^6-cyclopropyl-2-phenyl **7** containing the optimal sulfamide linkages were prepared in an effort to increase the lipophilicity (Scheme 2). These individual modifications on a sulfamate template were previously shown to improve potency and selectivity.[34] For the synthesis of **6** we explored a complimentary synthetic route (**19**→**20**→**21**→**22**→**6**) employing sulfamoylation with the novel dimethylaminopyridinium-activated reagent **30** as reported by Tan and co-workers.[44] N^6-Cyclopropyl-2′,3′-*O*-isopropylideneadenosine **19**[34] was elaborated to 5′-amino derivative **20** through sequential azidation and hydrogenation. Sulfamoylation of aminonucleoside **20** was achieved with dimethylaminopyridinium-activated **30**[44] followed by deprotection of the Cbz group to give the free sulfamide **21** that was converted to **6** through sequential salicylation and global deprotection using the standard conditions developed for **4**. N^6-cyclopropyl-2-phenyl **7** was prepared from **23** in analogy to **4** (**23**→**24**→**25**→**7**).

To complete our narrative, we explored fluorinated analogs **8**–**10**, since fluorine is known to affect absorption-distribution-metabolism-excretion (ADME) properties.[45] The enhanced PK parameters of **8** prompted the synthesis of **9**–**10** (*vide infra*). Fluorinated analog **8** was prepared from **26** in analogy to **4** (**26**→**27**→**28**→**8**) as presented in Scheme 2. The synthesis of 2′-fluoro-2-phenyl analog **9** is illustrated in Scheme 3 starting from commercially available 2′-deoxy-2′-fluoroguanosine **33**. Acetylation of the 3' and 5' alcohols provided **34**, which was transformed to **35** by sequential chlorination employing $POCl_3$ in dimethylaniline (DMA) promoted by Et_4NCl followed by Sandmeyer-like reaction with isoamyl nitrite and diiodomethane.[46, 47] Ammonolysis yielded adenosine derivative **36** that was immediately *tert*-butyldimethylsilyl (TBS) protected to provide **37**. The requisite C-2 phenyl group was incorporated by Buchwald-Hartwig coupling with phenylboronic acid to

give **38**.[48] Regioselective monodesilylation of the 5′ TBS group with AcOH–THF–H_2O (9:1:1) afforded the key nucleoside intermediate **39**. For installation of the sulfamide, we turned to new chemistry developed in our lab, which involves treatment of a 5′-aminonucleoside with sulfamide ($NH_2SO_2NH_2$), inspired by a side-reaction reported by Takai and co-workers.[49] In the present synthesis this was achieved by conversion of the 5′-alcohol in **39** to azide **40**. The azide was reduced by catalytic hydrogenation to provide a crude amine that was not isolated, but treated directly with sulfamide in dioxane at 90 °C to cleanly afford **41** in 87% yield. This new sulfamide synthesis is high yielding, experimentally simpler than our Mitsunobu protocol since it avoids contamination with triphenylphosphine oxide, and obviates N^6-protection on the nucleoside. The completion of the synthesis was accomplished using our standard salicylation method with **31** followed by TBS deprotection to furnish **9**.

Based on the improved PK properties of 2′-fluoro analog **8** (*vide infra*), we also pursued the synthesis of 2′,3′-dideoxy-2′-fluoro derivative **10**. Synthesis commenced from 2′-deoxy-2′-fluoroadenosine **42** that was regioselectively TBS protected at the C-5' alcohol to furnish **43**.[50] Barton-McCombie deoxygenation was accomplished in two steps through conversion to the corresponding thionocarbonate **44** followed by treatment with Bu_3SnH in refluxing toluene to yield **45**.[50] Deprotection of the TBS group with TFA provided alcohol **46**, which was transformed to azide **47** using methodology reported by Liu and Austin.[51] The sulfamide moiety at C-5' in **48** was then installed using our new protocol described in the previous section through azide reduction of **47** and in situ sulfamoylation of the crude aminonucleoside. The standard salicylation and TFA mediated deprotection sequence yielded the final analog **10**.

Enzyme Inhibition and Antitubercular Activity

The new analogs **5**–**10**, excluding the prodrugs **2** and **3**, were evaluated for enzyme inhibition against recombinant MbtA under initial velocity conditions as previously described (see Experimental Section).[32] The apparent inhibition constants (appK_i) were determined by fitting the concentration–response plots to the Morrison equation (eq 1, see Experimental Section) since all compounds exhibited tight-binding behavior (i.e. appK_i ≤10 × [MbtA]). The appK_i values for all analogs were potent, ranging from 0.78–8.9 nM (Table 1). These results are largely in agreement with prior findings and indicate that our targeted modifications to **1** did not adversely impact potency.

Next, we evaluated the new analogs against whole-cell *M. tuberculosis* H37Rv under iron-deficient conditions as previously described.[28] The minimum inhibitor concentrations (MIC) that resulted in complete inhibition of observable growth are shown in Table 1. Notably, all new analogs **5**–**10** retained fairly potent antitubercular activity with MIC values ranging from 0.098– 6.25 μM. Good correlation between appK_i and MIC values was observed for **1, 4, 6** and **8** with the MIC/appK_i ratio (both units in μM) varying only slightly with the median ratio of 72 ± 16 for these four compounds. However, the relative whole-cell activity for 3′-deoxy-2′-fluoro **10**, *p*-aminosalicyl **5**, and 2′-fluoro-2-phenyl **9** was eroded, with the MIC increasing to 0.78–3.125 μM despite potent enzyme inhibition. This is reflected in the MIC/appK_i ratios of 260, 351 and 975, respectively. The most deleterious modification was found

in the di-functionalized N^6-cyclopropyl-2-phenyl derivative **7**, whose MIC of 6.25 μM is nearly 10,000-fold greater than the appK_i.

Pharmacokinetic Analysis

All compounds were evaluated in a crossover experiment employing doubly cannulated female Sprague-Dawley rats to determine pharmacokinetic parameters. While mice are normally used for these studies, we elected to use rats based on the ability to serially sample a single animal and perform oral and intravenous crossover studies, which greatly minimized inter-animal variability. Each compound was orally dosed (*p.o.*) at 25 mg/kg in three rats, and sampling was conducted at the indicated time points (see Experimental Section). After a three-day washout period, each rat was then dosed intravenously (*i.v.*) at 2.5 mg/kg as a single bolus with more intensive sampling at early time points (see Experimental Section). Pharmacokinetic parameters shown in Table 2 were calculated from concentration-time profiles by non-compartmental analysis. From these studies, the area under the concentration-time curve (AUC) for each dose and absolute oral bioavailability (F) were determined. Additional relevant parameters that will be discussed are the maximum serum concentration (C_{max}) for the *p.o.* dose and the terminal elimination half-life ($t_{1/2}$) and clearance (CL) for the *i.v.* dose. We began our studies by administering a known antitubercular agent, isoniazid (INH). The obtained PK parameters were consistent with several published studies of INH oral dosing and detection in rat plasma.[52, 53] INH was rapidly eliminated with a $t_{1/2}$ of 19 min and achieved a C_{max} of 13.5 μg/mL, which translated to a 65% oral bioavailability. Our minimal target PK candidate profile would provide an oral bioavailability of 20%, C_{max} at least 50-fold greater than the MIC, and a $t_{1/2}$ greater than 1 hour.

PK results of 1 and prodrugs—Following an oral dose, **1** reached a maximum serum concentration (C_{max}) of 0.4 μg/mL at 60 minutes with an AUC value of 66 min·μg/mL (Table 2). To determine the absolute bioavailability (F), **1** was then dosed *i.v.* to provide an AUC of 519 min·μg/mL that yielded an oral bioavailability of 1.3%. The terminal elimination half-life and clearance were 11 min and 4.9 mL/min·kg, respectively, indicating rapid elimination. While these results were discouraging, we note the maximum serum concentration (C_{max}) achieved is nearly two times the MIC value. The PK parameters obtained herein are nearly identical to those obtained in BALB/c mice (C_{max} = 1.2 μg/mL and AUC = 58.6 min·μg/mL) validating the Sprague-Dawley rat PK model as a practical surrogate for the murine PK model.

Microsomal stability studies with mouse, rat, and human microsomes demonstrated **1** is extremely stable to oxidative metabolism ($t_{1/2}$ > 30 min) and is not glucuronidated (0% glucuronide detected at 60 min). The intra-molecular hydrogen-bonding of the phenol with the sulfamate nitrogen could account for the lack of observed glucuronidation. Moreover, **1** is highly water soluble (>50 mg/mL) and stabile under both acidic (pH 1) and alkaline (pH 12) conditions showing less than 5% degradation after 24 h at 37 °C. Collectively, these results suggest renal clearance of this highly polar nucleoside as the likely elimination mechanism. We also assessed the membrane permeability using the Caco-2 monolayer model to provide a benchmark for other analogs. These studies indicate moderate

permeability with a flux ($P_{app(A\ to\ B)}$) of 1.2×10^{-6} cm/s, and a favorable efflux ratio of 0.78 (Table 3).

The acetate prodrugs **2** and **3** were dosed orally, but neither of the parent compounds was detected in the serum samples and only a negligible amount of **1** could be detected with **3**. Serum stability studies of tri-acetate **3** (see Figure S8) indicated the phenol acetate was rapidly cleaved to liberate di-acetate **2**, which was slowly hydrolyzed to **1**. Caco-2 studies with **2** showed a reduced transport rate ($P_{app(A\ to\ B)}$) of 6.2×10^{-7} cm/s, which is approximately 50% of **1**, as well as an efflux ratio of 1.55 that is twice that of **1** (Table 3).

Modulation of the Sulfamate pK_a—Our next attempt to enhance oral exposure involved modulation of the pK_a of the charged linker in **1**, whose estimated pK_a is ∼3 based on the experimentally determined value for a related analogue.[28] This acidic functional group is expected to be ionized under physiological conditions, which may impede membrane transport, thus analogs with pK_a values closer to 7 would be desirable. Replacement of the sulfamate linkage with the sulfamide linkage in **4** is predicted to raise the pK_a to ∼5 while installation of the electron-donating *para*-amino group in **5** is expected to further raise the pK_a to ∼6.[28] Sulfamide **4** achieved a C_{max} of 0.7 μg/mL or 1.4 μM, which is 7-fold higher than the MIC. The oral exposure ($AUC_{p.o.}$) was increased 50% to 100 min·μg/mL that led to a nearly 3-fold improved bioavailability of 3.5%. Caco-2 studies of **4** did not indicate enhanced permeability since the $P_{app(A\ to\ B)}$ relative to **1** was unchanged, while the efflux ratio was nearly identical (Table 3). Based on this modest improvement all subsequent analogs were prepared with the sulfamide linkage.

The *para*-amino analog **5** was then evaluated. Unfortunately, this compound had significantly lower oral exposure with an $AUC_{p.o.}$ of only 17 min·μg/mL, and reached a C_{max} of 0.09 μg/mL, which is far below the MIC value. The *i.v.* exposure was also diminished, and can be attributed to the substantially faster clearance of 46.4 mL/min·kg, which is nearly 10-fold greater than **1**, and the highest value of any analog in this series. The enhanced clearance of **5** is likely caused by the increased polarity of this molecule due to introduction of the *para*-amino group.

Impact of Lipophilicity—To evaluate the impact of lipophilicity on absorption, we evaluated N^6-cyclopropyl **6** and N^6-cyclopropyl-2-phenyl **7**. These modifications increased the clogP values from −0.89 for compound **1** to 0.5 and 2.9, respectively. The C_{max} for both analogs ranged from 0.1 to 0.14 μg/mL while the $AUC_{p.o.}$ values ranged from 4 to 19 min·μg/mL, indicating low oral exposure. The half-life of both compounds marginally improved to 15 min. The oral bioavailability of **6** was unchanged relative to **1** while the oral bioavailability of **7** was a dismal 0.3%. The increased lipophilicity of **7** manifested as poor aqueous solubility and several excipients (carboxymethylcellulose, 25% hydroxypropyl-β-cyclodextrin, and 50% PEG400–5% tween-80) were evaluated to potentially improve oral absorption without success. These results suggest that enhancing the lipophilicity through addition of nonpolar groups is detrimental to improving PK. In retrospect, the high molecular weight (MW) of **1** leaves little room to maneuver, and both **6** and **7** exceed Lipinski's threshold MW value of 500. The permeability of **7** as measured using Caco-2 cell

studies corroborate the low bioavailability and indicate low permeability with a flux of 5.2 × 10^{-7} cm/s, about two-fold less than either **1** or **4**, and an efflux ratio of 3.45.

Fluorinated Analogs—Fluorine is commonly used to improve drug properties and can increase oral exposure through reduction of cytochrome P450-mediated metabolic clearance. Fluorination at the C-2' position of nucleosides is also known to enhance anomeric stability, which can lead to an improved PK profile if degradation by cleavage of the anomeric linkage occurs at acidic pH.[54] Introduction of a fluorine at the C-2' position in **8** led to a nearly 3-fold increase in oral exposure relative to **1**, with an $AUC_{p.o.}$ of 188 min·μg/mL that is concordant with a 3-fold increase in half-life to 32.5 min (relative to 11 min for **1**). Since the $AUC_{i.v.}$ is also dramatically increased to 1043 min·μg/mL due to the increased half-life, the oral bioavailability remains low at 2%. Caco-2 studies of **8** demonstrated enhanced permeability with a flux of 4.2 × 10^{-6} cm/s, or nearly 4-fold greater than **1** and **4**, and a favorable efflux ratio of 0.32 (Table 3). Unfortunately, this did not translate to improved bioavailability, as noted above, and suggests a limitation of the Caco-2 *in vitro* model for predicting oral bioavailability for this compound class. The 2′-fluoro-2-phenyl **9** showed a dramatic improvement in half-life to 121 min, which is 11-fold greater than **1**, and resulted in an astonishing *i.v.* exposure of 1981 min·μg/mL. Unfortunately, the oral exposure ($AUC_{p.o.}$) was diminished relative to **8**, but still 2-fold greater than **1**. The oral bioavailability therefore remained low at 0.8%. 2′,3′-Dideoxy-2′-fluoro **10** was the last compound evaluated with the anticipation that removal of the polar 3′-hydroxyl group may enhance membrane permeability. Compound **10** indeed realized the highest oral exposure with an $AUC_{p.o.}$ of 198 min·μg/mL and a C_{max} of 0.56 μg/mL. Additionally, the half-life was improved to 62 min, but the oral bioavailability remained unchanged relative to **8**. Overall, these results demonstrate that replacement of the 2′-hydroxyl group with a fluorine atom results in a dramatically enhanced half-life, which translates to improved oral exposure.

Conclusion

Four complimentary strategies were examined to improve the drug disposition and pharmacokinetic properties of a new class of antibiotics that inhibit siderophore biosynthesis in *M. tuberculosis*. Our first approach involved preparation of simple di- and tri-acetate prodrugs (**2** and **3**) to mask the polar hydroxyl groups of the prototypical inhibitor **1**. Unfortunately, neither prodrug was orally bioavailable. Plasma stability studies suggested rapid cleavage of **3** to **2** that underwent slow cleavage to afford **1**. Alternate pro-moieties with faster cleavage kinetics could be explored to mask the 2′ and 3′ hydroxyls. The complete lack of oral exposure with **2** and **3** suggested this would not be a viable strategy and further studies along this line were not pursued.

We hypothesized that the ionized acyl-sulfonyl linker of the adenylation inhibitors described herein may impede membrane permeability. The negative charge is required for potent binding due to critical electrostatic interactions in the active site of MbtA and any attempts to remove this charge have resulted in complete loss of activity.[28] Thus, we designed analogs to increase the pK_a of the acyl-sulfonyl nitrogen linker. The sulfamide analog **4** possessed 3-fold improved bioavailability relative to **1**, as well as 50% increased oral

exposure and a more than 3-fold higher C_{max}/MIC ratio. Incorporation of a *para*-amino group on the salicyl moiety in **5** led to a significant loss in oral exposure. This is attributed to dramatically enhanced clearance caused by the additional polar amino group. Given the modest improvements realized with this approach, coupled with the strict requirements for an acyl-sulfonyl linker moiety from our prior extensive SAR studies, further modifications to the salicyl moiety were not pursued. Moreover, we later recognized these salicyl-nucleoside analogs can engage in intramolecular hydrogen bonding between the sulfonyl nitrogen and the *ortho*-phenol of the salicyl moiety. This could partially shield the polarity through delocalization of the charge and mitigate our initial concerns about the ionized acyl-sulfonyl linker.[55]

The third approach to enhance ADME and PK properties involved modulation of the lipophilicity. While it is recognized that many antibacterials have unique physicochemical properties relative to other drug classes, we nevertheless sought to increase the lipophilicity of the highly polar nucleoside derivative **1**.[56] This was achieved through addition of non-polar groups onto the nucleoside at sites previously shown to enhance biochemical potency and antibacterial activity.[34] The calculated logP of N^6-cyclopropyl **6** and N^6-cyclopropyl-2-phenyl **7** was increased to +0.5 and +2.9, respectively. However, both compounds realized dramatically lower oral exposures and failed to even reach a C_{max} exceeding their MIC values. A more fruitful approach to increasing lipophilicity may be through strategic deletion of polar functional groups and atoms that are dispensable for activity, as this would additionally result in a reduction of the molecular weight.

Incorporation of a fluorine atom at C-2′ of the nucleoside in analogs **8–10** led to the most pronounced improvements in oral exposure, primarily through an increase in the terminal elimination half-life ($t_{1/2}$) following *i.v.* administration from 11 minutes for **1** to 32–121 minutes for **8–10**. The apparent terminal elimination half-lives following oral dosing for all of the compounds described herein are much longer, presumably due to slow absorption, and do not reflect the rate of elimination. To calibrate these values, the intrinsic half-life of the first-line antitubercular agent isoniazid in a rat is only 18 minutes. Fluorine is commonly introduced to enhance $t_{1/2}$ through blocking P450-mediated metabolism.[45] In the case of nucleosides, a C-2′ fluoro group improves the stability of the anomeric linkage, which can be important for some nucleosides that degrade by anomeric cleavage under the acidic conditions of gastric fluids.[54] We have shown **1** and its derivatives to be extremely stable under strongly acidic conditions, while microsomal stability studies revealed little metabolism of **1**. Thus, we hypothesize that the C-2′ fluoro group likely decreases renal clearance.

In order to provide an *in vitro* marker for oral bioavailability, we also measured select analogs using the standard Caco-2 model system for intestinal epithelial permeability. These experiments showed the Caco-2 model may be qualitatively useful, but is not quantitatively predictive of oral bioavailability. We identified a minimum threshold $P_{app(A\ to\ B)}$ of 1×10^{-6} cm/s that can now be used to eliminate candidates prior to PK evaluation.

Through logical modification of **1** we explored multiple strategies to enhance pharmacokinetic parameters, and successfully increased the intrinsic half-life and oral

exposure. While were unable to reach our minimal target PK candidate profile, we believe these studies have provided a foundation to more effectively address the PK limitations of **1**. Our findings may also be applicable to other adenylation inhibitors, which have been described for dozens of other functionally related adenylating enzymes involved in diverse disease processes.[57, 58]

EXPERIMENTALS

General materials and methods

Chemicals and solvents were purchased from Acros Organics, Alfa Aesar, Sigma-Aldrich, and TCI America and were used as received. The nucleosides 2′-deoxy-2′-fluoroguanosine **33** and 2′-deoxy-2′-fluoroadenosine **42** were obtained from Metkinen Chemistry (Kuopio, Finland). Compounds **1**,[28] **11**,[39] **14**,[39] **19**,[34] **23**,[35] **26**,[59] **27**,[59] **29**,[40] **30**,[44] **31**,[32] **32**,[43] and *N*-hydroxysuccinimidyl 2-benzyloxybenzoate[28] were prepared as described. All final compounds (**1–10**) were purified by preparative reverse-phase HPLC using the indicated method and purity (≥95%) of the lyophilized powders was confirmed by analytical reverse-phase HPLC. An anhydrous solvent dispensing system using two packed columns of neutral alumina was used for drying THF and CH_2Cl_2, while two packed columns of molecular sieves were used to dry DMF, and the solvents were dispensed under argon gas (Ar). Anhydrous grade MeOH, MeCN, pyridine, and DMA were purchased from Aldrich. EtOAc and hexanes were purchased from Fisher Scientific. All reactions were performed under an inert atmosphere of dry argon gas (Ar) in oven-dried (180 °C) glassware. TLC analyses were performed on TLC silica gel 60F254 plates from EMD Chemical Inc. and were visualized with UV light. Purification by flash chromatography was performed using a medium-pressure flash chromatography system equipped with flash column silica cartridges with the indicated solvent system. Reversed-phase HPLC (RP-HPLC) purification was performed on Phenomenex Gemini 10 μm C18 columns (250 × 21.2 or 10 or 4.6 mm) with detection at 254 nm employing the indicated solvent system. ^{1}H and ^{13}C spectra were recorded on a 400 or 600 MHz Varian, or 700 MHz Bruker NMR spectrometer. Proton chemical shifts are reported in ppm from an internal standard of residual chloroform (7.26), methanol (3.31), dimethyl sulfoxide (2.50), or mono-deuterated water (HDO, 4.79); carbon chemical shifts are reported in ppm from an internal standard of residual chloroform (77.0), methanol (49.1), or dimethyl sulfoxide (39.5). Proton chemical data are reported as follows: chemical shift, multiplicity (s = singlet, d = doublet, dt = doublet of triplets, t = triplet, q = quartet, pentet = pent, m = multiplet, ap = apparent, br = broad, ovlp = overlapping), coupling constant(s), integration. High-resolution mass spectra were obtained on an LTQ Orbitrap Velos (Thermo Scientific, Waltham, MA).

General Procedure for Mitsunobu Reaction

To a solution of nucleoside (1.0 equiv), **29** (3.0 equiv) and PPh_3 (1.05 equiv) in THF (0.05 M for limiting reagent) at 0 °C was added neat DIAD (1.05 equiv) dropwise over 15 min. The solution was stirred at 0 °C for 45 min, then gradually warmed to 23 °C over 3 h and stirred for 12 h at 23 °C. The reaction was concentrated under reduced pressure to a dark yellow oil and immediately purified by flash chromatography (linear gradient 0–100% EtOAc–hexanes) to afford the title compound.

General Procedure for Salicylation

To a solution the sulfamide nucleoside (1.0 equiv) and Cs_2CO_3 (2.5 equiv) in DMF (0.5 M for limiting reagent) at 0 °C was added **31** (1.5 equiv). The reaction mixture was then stirred for 24 h at 23 °C during which time all starting material was consumed as monitored by electrospray mass spectrometry in the negative mode. DMF was removed by rotary evaporation under high vacuum (P = 0.01 torr) to afford crude salicylated nucleoside. The crude product was used in the next global deprotection reaction directly without further purification.

General Procedure for TFA Global Deprotection

To a solution of the crude salicylated nucleoside in H_2O (10 mL/mmol) at 0 °C was added TFA (40 mL/mmol) dropwise (final concentration 0.02 M). The reaction mixture was stirred for 8 h at 23 °C during which time all starting material was consumed as monitored by electrospray mass spectrometry in the negative mode. The solvent was removed under vacuum. The crude material was re-dissolved in 1:1 MeCN–50 mM TEAB (10–20 mg/mL) and filtered to remove insoluble solids. The resulting solution was purified by reverse phase HPLC employing the indicated method and column using 50 mM aqueous triethylammonium bicarbonate (TEAB) at pH 7.5 (solvent A) and acetonitrile (solvent B). The appropriate fractions were pooled and lyophilized to afford the final compound as the triethylammonium salt as a white foam.

5′ -*O*-[*N*-(2-Benzyloxybenzoyl)sulfamoyl]-N^6,N^6-bis(*tert*-butyloxycarbonyl)-2′, 3′ -*O*-isopropylideneadenosine triethylammonium salt (12)

To a stirring solution of **11** (0.54 g, 0.92 mmol, 1.0 equiv) in DMF (9.2 mL) cooled to 0 °C was added *N*-hydroxysuccinimidyl 2-benzyloxybenzoate (0.45 g, 1.38 mmol, 1.5 equiv) followed by Cs_2CO_3 (0.60 g, 1.84 mmol, 2.0 equiv) and the mixture was stirred at 23 °C for 21 h. The crude reaction mixture was concentrated under reduced pressure to a yellow oil that was taken up in EtOAc (200 mL) and filtered. The precipitate was washed with additional EtOAc (200 mL), and the combined filtrate was concentrated under reduced pressure and purified by flash chromatography (linear gradient 0–5% MeOH/EtOAc with 1% Et_3N) to afford the title compound (0.51 g, 62%) as a white foamy oil: R_f = 0.37 (1:9 MeOH–EtOAc with 1% Et_3N); ^{1}H NMR (600 MHz, CD_3OD) δ 1.13 (t, *J* = 7.2 Hz, 9H), 1.35 (s, 3H), 1.40 (s, 18H), 1.61 (s, 3H), 2.83 (q, *J* = 7.2 Hz, 6H), 4.19–4.20 (m, 2H), 4.41 (dd, *J* = 6.0, 3.6 Hz, 1H), 5.12–5.13 (m, 3H), 5.38 (dd, *J* = 6.0, 3.6 Hz, 1H), 6.37 (d, *J* = 3.0 Hz, 1H), 6.95 (t, *J* = 7.8 Hz, 1H), 7.05 (d, *J* = 8.4 Hz, 1H), 7.25 (t, *J* = 7.8 Hz, 1H), 7.31–7.34 (m, 3H), 7.46 (d, *J* = 7.8 Hz, 1H), 7.52 (d, *J* = 7.2 Hz, 2H), 8.84 (s, 1H), 8.89 (s, 1H); ^{13}C NMR (150 MHz, CD_3OD) δ 10.2, 25.7, 27.8, 28.2, 47.4, 69.8, 71.6, 83.1, 85.4, 86.0, 86.2, 92.5, 115.3, 121.3, 121.9, 128.9, 129.2, 129.3, 129.6, 129.9, 130.3, 131.7, 131.9, 138.7, 146.8, 151.2, 151.7, 153.3, 154.6, 157.2, 176.9; HRMS (ESI–) calcd for $C_{37}H_{43}N_6O_{12}S$ $[M - H]^-$ 795.2665, found 795.2659 (0.8 ppm error).

2′, 3′ -*O*-di-Acetyl-5′ -*O*-[*N*-(2-hydroxybenzoyl)sulfamoyl]adenosine (2)

To a flask containing **12** (0.51 g, 0.56 mmol, 1.0 equiv) at 0 °C was added 80% aqueous TFA (6 mL) that had also been cooled to 0 °C and the mixture stirred at 0 °C for 1 h then at

23 °C for 3 h. The reaction mixture was concentrated under reduced pressure to a yellow oil and dried under high vacuum to remove all traces of TFA, then dissolved in DMF (6 mL) to which was added pyridine (0.17 mL, 2.1 mmol, 3.8 equiv) followed by acetic anhydride (0.33 mL, 3.5 mmol, 6.4 equiv) and the mixture stirred at 23 °C for 16 h. The reaction was concentrated under reduced pressure to remove all traces of DMF and give **13** as a crude yellow oil that was used directly in the next step without purification.

To a round-bottomed flask containing the crude product **13** prepared above (0.25 g, 0.33 mmol, 1.0 equiv) purged with argon was added anhydrous MeOH (3.4 mL) followed by Pd/C (0.030 g, 10% by weight) and the flask evacuated by house vacuum and back-filled with an H_2 balloon 3 times before being allowed to stir vigorously under an H_2 balloon at 23 °C for 2 h. The crude reaction mixture was filtered over a pad of Celite and concentrated under reduced pressure to a dark oil. Purification by semi-preparative reverse-phase HPLC on a Phenomenex Gemini 10 μm C18 (250 × 10.0 mm) column at a flow rate of 5 mL/min with isocratic elution of 35% MeCN–50 mM aqueous triethylammonium bicarbonate for 10 min, followed by 70% MeCN for 5 min. The retention time of the product was 5.4 minutes (k' = 1.2) and the appropriate fractions were pooled and lyophilized to afford the title compound (90.0 mg, 42%) as a white solid: R_f = 0.18 (1:9 MeOH–CH_2Cl_2 with 1% Et_3N); ^{1}H NMR (600 MHz, CD_3OD) δ 1.23 (t, *J* = 7.2 Hz, 9H), 2.00 (s, 3H), 2.10 (s, 3H), 3.03 (q, *J* = 7.2 Hz, 6H), 4.44 (dd, *J* = 12.0, 3.0 Hz, 1H), 4.47 (dd, *J* = 11.4, 3.6 Hz, 1H), 4.53 (q, *J* = 3.6 Hz, 1H), 5.70 (dd, *J* = 5.4, 3.6 Hz, 1H), 5.89 (t, *J* = 6.0 Hz, 1H), 6.27 (d, *J* = 6.6 Hz, 1H), 6.75–6.79 (m, 2H), 7.28 (t, *J* = 7.2 Hz, 1H), 7.93 (d, *J* = 7.8 Hz, 1H), 8.18 (s, 1H), 8.56 (s, 1H); ^{1}H NMR (600 MHz, DMSO-d_6) δ 1.17 (t, *J* = 7.2 Hz, 9H), 1.99 (s, 3H), 2.10 (s, 3H), 3.09 (q, *J* = 7.2 Hz, 6H), 4.25 (dd, *J* = 11.4, 4.8 Hz, 1H), 4.33 (dd, *J* = 11.4, 4.2 Hz, 1H), 4.44 (q, *J* = 4.2 Hz, 1H), 5.56 (dd, *J* = 5.4, 4.2 Hz, 1H), 5.90 (t, *J* = 6.0 Hz, 1H), 6.20 (d, *J* = 6.0 Hz, 1H), 6.72–6.75 (m, 2H), 7.26 (t, *J* = 7.2 Hz, 1H), 7.36 (br s, 2H), 7.81 (d, *J* = 7.8 Hz, 1H), 8.14 (s, 1H), 8.46 (s, 1H), 13.5 (s, 1H); ^{13}C NMR (150 MHz, CD_3OD) δ 9.9, 20.3, 20.6, 47.8, 69.1, 73.0, 75.3, 82.7, 87.1, 118.0, 119.4, 120.2, 120.7, 131.6, 134.5, 141.3, 150.8, 154.2, 157.5, 162.3, 171.0, 171.5, 175.3; HRMS (ESI–) calcd for $C_{21}H_{21}N_6O_{10}S$ $[M - H]^-$ 549.1045, found 549.1048 (0.5 ppm error).

5′-*O*-[*N*-(2-Acetoxybenzoyl)sulfamoyl]-2′, 3′-*O*-di-acetyladenosine (3)

To a stirring solution of **1** (0.10 g, 0.18 mmol, 1.0 equiv) in DMF was added pyridine (0.05 mL, 0.68 mmol, 3.8 equiv) followed by acetic anhydride (0.11 mL, 1.13 mmol, 6.4 equiv) and the mixture stirred at 23 °C for 21 h. The crude reaction mixture was concentrated under reduced pressure to a yellow oil and purified by flash chromatography (linear gradient 0–5% MeOH/DCM with 1% Et_3N) to afford an approximately 5:1 mixture of **3** and **2**. The desired compound was purified by semi-preparative reverse-phase HPLC on a Phenomenex Gemini 10 μm C18 (250 × 10.0 mm) column at a flow rate of 5 mL/min with a linear gradient 20–70% MeCN–50 mM aqueous triethylammonium bicarbonate for 10 min, followed by 70% MeCN for 5 min. The retention time of the product was 6.6 minutes (k' = 1.6) and the appropriate fractions were pooled and lyophilized to afford the title compound (57.8 mg, 46%) as a white solid: R_f = 0.25 (1:9 MeOH– CH_2Cl_2 with 1% Et_3N); ^{1}H NMR (600 MHz, CD_3OD) δ 1.27 (q, *J* = 7.2 Hz, 9H), 2.00 (s, 3H), 2.13 (s, 3H), 2.26 (s, 3H), 3.17 (t, *J* = 6.0 Hz, 6H), 4.40 (dd, *J* = 14.4, 3.6 Hz, 1H), 4.44 (dd, *J* = 9.6, 3.0 Hz, 1H), 4.54 (d, *J* = 3.0 Hz,

1H), 5.70–5.71 (m, 1H), 5.89 (t, *J* = 6.0 Hz, 1H), 6.29 (d, *J* = 6.0 Hz, 1H), 7.02 (d, *J* = 7.8 Hz, 1H), 7.06 (s, 1H), 7.23 (t, *J* = 7.8 Hz, 1H), 7.41 (t, *J* = 7.2 Hz, 1H), 7.86 (d, *J* = 7.8 Hz, 1H), 8.19 (s, 1H), 8.59 (s, 1H); ^{13}C NMR (150 MHz, CD_3OD) δ 9.4, 20.3, 20.6, 21.4, 48.0, 69.1, 73.2, 75.3, 82.9, 87.0, 120.2, 124.1, 126.7, 131.9, 132.2, 133.1, 141.3, 150.8, 150.9, 154.2, 157.2, 171.0, 171.5, 172.0, 173.8; HRMS (ESI–) calcd for $C_{23}H_{23}N_6O_{11}S$ $[M - H]^-$ 591.1151, found 591.1170 (3.2 ppm error).

N^6,*N*^{6}-bis(*tert*-Butoxycarbonyl)-5′-*N*-[*N*-(*tert*-butoxycarbonyl)-*N*-sulfamoyl]amino-5′-deoxy-2′, 3′-*O*-isopropylideneadenosine (15)

The title compound was prepared from **14** (0.60 g, 1.2 mmol) using the general procedure for the Mitsunobu reaction and isolated as a foamy oil (0.789 g, 96%): R_f = 0.25 (1:1 EtOAc–hexanes); ^{1}H NMR (600 MHz, $CDCl_3$) δ 1.40 (s, 21H), 1.46 (s, 9H), 1.49 (s, 3H), 1.61 (s, 3H), 3.94 (dd, *J* = 15.0, 7.8 Hz, 1H), 3.99 (dd, *J* = 15.6, 5.4 Hz, 1H), 4.51 (p, *J* = 4.8 Hz, 1H), 4.90 (p, *J* = 6.0 Hz, 1H), 5.24 (dd, *J* = 6.0, 3.6 Hz, 1H), 5.57 (dd, *J* = 6.0, 1.8 Hz, 1H), 6.38 (d, 1H, 1.8 Hz), 8.64 (s, 1H), 8.88 (s, 1H); ^{13}C NMR (150 MHz, $CDCl_3$) δ 27.6, 28.2, 28.4, 28.5, 49.9, 83.6, 85.1, 85.4, 85.6, 87.5, 91.6, 115.6, 130.7, 147.6, 151.1, 151.5, 153.1, 153.2, 154.2; HRMS (ESI–) calcd for $C_{28}H_{42}N_7O_{11}S$ $[M - H]^-$ 684.2668, found 684.2685 (2.5 ppm error).

N^6,*N*^{6}-bis(*tert*-Butoxycarbonyl)-5′-*N*-(*N*-*tert*-butoxycarbonyl-*N*-{[(2-*O*-methoxymethoxy)benzoyl]sulfamoyl})amino-5′-deoxy-2′, 3′-*O*-isopropylideneadenosine triethylammonium salt (16)

The title compound was prepared from **15** (0.52 g, 0.75 mmol, 1.0 equiv) using the general procedure for salicylation and isolated as an off-white amorphous solid (0.38 g, 53%): R_f = 0.37 (1:9 MeOH–CH_2Cl_2 with 1% Et_3N); ^{1}H NMR (600 MHz, $CDCl_3$) δ 1.26 (t, *J* = 7.2 Hz, 9H), 1.37 (s, 3H), 1.39 (s, 18H), 1.45 (s, 9H), 1.62 (s, 3H), 3.11 (q, *J* = 7.2 Hz, 6H), 3.45 (s, 2H), 4.06 (dd, *J* = 15.0, 6.0 Hz, 1H), 4.64 (dd, *J* = 18.0, 7.2, Hz, 1H), 4.60–4.63 (m, 1H), 5.14 (s, 2H), 5.28 (dd, *J* = 6.0, 3.0 Hz, 1H), 5.51 (dd, *J* = 6.6, 3.0 Hz, 1H), 6.32 (d, 2.4 Hz, 1H), 6.96 (t, *J* = 7.2 Hz, 1H), 7.11 (d, *J* = 8.4 Hz, 1H), 7.27 (t, *J* = 7.8 Hz, 1H), 7.51 (d, *J* = 7.8 Hz, 1H), 8.74 (s, 1H), 8.89 (s, 1H); ^{13}C NMR (150 MHz, $CDCl_3$) δ 7.9, 27.7, 28.0, 46.1, 52.8, 56.3, 63.3, 81.4, 82.3, 83.7, 84.5, 85.0, 90.3, 96.5, 114.3, 118.0, 121.9, 129.0, 129.8, 131.3, 144.0, 150.0, 150.3, 151.6, 152.2, 152.5, 153.0, 154.5; HRMS (ESI–) calcd for $C_{37}H_{50}N_7O_{14}S$ $[M - H]^-$ 848.3142, found 848.3146 (0.5 ppm error).

5′-*N*-[*N*-(2-Hydroxybenzoyl)sulfamoyl]amino-5′-deoxyadenosine triethylammonium salt (4)

The title compound was prepared (150 mg, 65%) from **16** (380 mg, 0.39 mmol) using the general procedure for TFA deprotection and purified by preparative-reverse phase HPLC as described. The analytical data (^{1}H NMR, ^{13}C NMR, HRMS) agreed with previously reported values for **4** obtained by an alternate synthetic route.[28]

5′-*N*-[*N*-(4-Benzyloxycarbonylamino-2-hydroxybenzoyl)-*N*-(*tert*-butoxycarbonyl)sulfamoyl]amino-N^6,N^6-bis(*tert*-butoxycarbonyl)-5′-deoxy-2′,3′-*O*-isopropylideneadenosine triethylammonium salt (17)

To a stirring solution of **32** (0.75 g, 2.6 mmol, 3.0 equiv) in DMF (4.4 mL) was added CDI (0.51 g, 3.2 mmol, 3.6 equiv) and the mixture heated at 60 °C for 2 h. The reaction mixture was cooled to 23 °C, and **15** (0.60 g, 0.87 mmol, 1.0 equiv) was added as a solution in DMF (4.4 mL) followed by solid Cs_2CO_3 (0.43 g, 1.31 mmol, 1.5 equiv), and stirred for 15 h. The crude reaction mixture was concentrated under reduced pressure to a dark oil and purified by flash chromatography (linear gradient 0–5% MeOH–CH_2Cl_2 with 1% Et_3N) to afford the title compound (0.46 g, 50%) as a waxy light yellow solid: R_f = 0.61 (1:9 MeOH–CH_2Cl_2 with 1% Et_3N); ^{1}H NMR (600 MHz, CD_3OD) δ 1.09 (t, *J* = 7.2 Hz, 9H), 1.36 (s, 9H), 1.38 (s, 18H), 1.40 (s, 3H), 1.61 (s, 3H), 2.67 (q, *J* = 7.2 Hz, 6H), 4.05 (dd, *J* = 15.0, 6.6 Hz, 1H), 4.18 (dd, *J* = 15.0, 7.2 Hz, 1H), 4.63 (td, *J* = 7.2, 3.0 Hz, 1H), 5.17 (s, 2H), 5.27 (dd, *J* = 5.4, 3.0 Hz, 1H), 5.57 (dd, *J* = 6.0, 3.0 Hz, 1H), 6.33 (d, *J* = 2.4 Hz, 1H), 6.82 (d, *J* = 9.0 Hz, 1H), 7.06 (s, 1H), 7.30 (d, *J* = 7.2 Hz, 1H), 7.36 (t, *J* = 7.8 Hz, 1H), 7.41 (d, *J* = 7.8 Hz, 1H), 7.75 (d, *J* = 8.4 Hz, 1H), 8.74 (s, 1H), 8.89 (s, 1H); ^{13}C NMR (150 MHz, CD_3OD) δ 10.9, 25.7, 27.7, 28.2, 28.5, 47.3, 53.8, 67.7, 83.8, 84.0, 85.4, 87.3, 92.1, 106.8, 109.9, 115.5, 116.0, 129.1, 129.3, 129.7, 130.7, 131.9, 134.6, 138.1, 145.0, 147.3, 151.2, 151.6, 153.3, 154.4, 154.5, 155.4, 162.4, 173.6; HRMS (ESI–) calcd for $C_{43}H_{53}N_8O_{15}S$ $[M - H]^-$ 953.3357, found 953.3328 (3.0 ppm error).

5′-*N*-[*N*-(4-Amino-2-hydroxybenzoyl)sulfamoyl]amino-5′-deoxyadenosine (5)

To a Parr flask purged with Ar was added **17** (0.50 g, 0.52 mmol, 1.0 equiv) dissolved in MeOH (5.2 mL) followed by Pd/C (0.05 g, 10% by weight). The flask was evacuated and back-filled with H_2 five times before filling the flask to 40 psi H_2 and shaking on a Parr shaker at 23 °C. After 1 h, the reaction was filtered over a pad of Celite and concentrated under reduced pressure to afford **18** as a colorless oil that was used directly in the next step without purification.

To a flask containing the crude **18** prepared above at 0 °C was added 80% aqueous TFA (5.2 mL) that had also been cooled to 0 °C. The reaction was stirred for 1 h at 0 °C, 12 h at 4 °C, and 5 h at 23 °C. The reaction was concentrated under reduced pressure to remove all traces of TFA. Purification by preparative reverse-phase HPLC on a Phenomenex Gemini 10 μm C18 (250 × 21.2 mm) column was achieved at a flow rate of 20 mL/min with a gradient of 5–25% MeCN–50 mM aqueous triethylammonium bicarbonate over 10 min, followed by 25% MeCN for 5 min. The retention time of the product was 9.0 minutes (k' = 2.0) and the appropriate fractions were pooled and lyophilized to afford the title compound (90 mg, 34%) as a white solid: ^{1}H NMR (600 MHz, CD_3OD) δ 1.20 (t, *J* = 7.2 Hz, 9H), 2.95 (q, *J* = 7.2 Hz, 6H), 3.29–3.31 (m, 2H), 4.23 (dd, *J* = 6.6, 4.2 Hz, 1H), 4.35 (dd, *J* = 5.4, 3.0 Hz, 1H), 4.85–4.86 (m, 1H), 5.93 (d, *J* = 6.6 Hz, 1H), 6.05 (s, 1H), 6.12 (d, *J* = 9.0 Hz, 1H), 7.62 (d, *J* = 9.0 Hz, 1H), 8.30 (s, 1H), 8.31 (s, 1H); ^{13}C NMR as determined by HMBC (150 MHz, CD_3OD) δ 10.1, 46.6, 47.7, 73.2, 75.0, 86.1, 90.6, 101.9, 107.4, 110.9, 120.9, 132.4, 142.0, 150.7, 154.3, 154.6, 157.5, 163.7, 175.0; HRMS (ESI-) calcd for $C_{17}H_{19}N_8O_7S$ $[M - H]^-$ 479.1103, found 479.1095 (1.7 ppm error).

5′-Amino-*N*^{6}-cyclopropyl-5′-deoxy-2′,3′-*O*-isopropylideneadenosine (20)

DIAD (3.4 mL, 17.3 mmol, 1.5 equiv) was dissolved in THF (300 mL) that had been cooled to 0 °C. Ph_3P (4.5 g, 17.3 mmol, 1.5 equiv) was added as a solution in THF (60 mL), and the solution stirred at 0 °C for 15 min. Compound **19** (4.0 g, 11.5 mmol, 1.0 equiv) was added as a solution in THF (60 mL), and the solution stirred at 0 °C for 15 min. DPPA (4.96 mL, 23.0 mmol, 2.0 equiv) was added directly and the solution stirred at 0 °C for 15 min then at 23 °C for 4.5 h. The reaction was quenched with H_2O (200 mL). The mixture was extracted with CH_2Cl_2 (3 × 200 mL), and the combined organic layers were dried over $MgSO_4$, filtered, and concentrated under reduced pressure to a clear oil that was dried under high vacuum for at least 4 h before being used directly in the next step.

To a Parr flask purged with Ar was added Pd/C (0.185 g, 10% by weight, added in 2 portions), followed by half the crude reaction mixture from above dissolved in anhydrous MeOH (50 mL). The flask was evacuated and back-filled with H_2 five times before filling the flask to 30 psi H_2 and shaking on a Parr shaker at 23 °C. After 1.75 h, the reaction was filtered over a pad of Celite, concentrated under reduced pressure to a dark oil, and purified by flash chromatography (linear gradient 0–10% MeOH–CH_2Cl_2). The same procedure was repeated with the second half of the crude reaction mixture to give the title compound (0.76 g, 44% over 2 steps) as a foamy oil: R_f = 0.05 (1:9 MeOH–CH_2Cl_2); ^{1}H NMR (600 MHz, CD_3OD) δ 0.61–0.64 (m, 2H), 0.85–0.88 (m, 2H), 1.35 (s, 3H), 1.57 (s, 3H), 2.92 (d, *J* = 5.4 Hz, 2H), 3.35 (s, 1H), 4.21–4.24 (m, 1H), 5.01 (dd, *J* = 6.6, 3.6 Hz, 1H), 5.46 (dd, *J* = 6.6, 3.0 Hz, 1H), 6.13 (d, *J* = 3.0 Hz, 1H), 8.21 (s, 1H), 8.28 (s, 1H); ^{13}C NMR (150 MHz, CD_3OD) δ 7.7, 25.7, 27.7, 44.6, 55.0, 83.3, 85.0, 88.3, 91.70, 91.71, 115.7, 121.4, 141.7, 154.0, 157.2; HRMS (ESI+) calcd for $C_{16}H_{23}N_6O_3$ $[M + H]^+$ 347.1826, found 347.1821 (1.4 ppm error).

N^6-Cyclopropyl-5′-deoxy-2′,3′-*O*-isopropylidene-5′-*N*-(sulfamoyl)aminoadenosine (21)

To a stirring solution of **20** (0.50 g, 1.4 mmol, 1.0 equiv) in CH_2Cl_2 (20 mL) was added **30** (0.63 g, 1.9 mmol, 1.3 equiv) and the mixture stirred at 23 °C for 14 h. The crude reaction was concentrated under reduced pressure to a foamy oil that was used directly in the next step.

To a Parr flask purged with Ar was added Pd/C (0.075 g, 10% by weight), followed by the crude reaction mixture from above dissolved in 2:1 MeOH–THF (15 mL). The flask was evacuated and back-filled with H_2 five times before filling the flask to 30 psi H_2 and shaking on a Parr shaker at 23 °C for 22 h. The reaction was filtered over a pad of Celite, concentrated under reduced pressure to a clear oil, and purified by flash chromatography (linear gradient 0–10% MeOH–CH_2Cl_2) to afford the title compound (0.35 g, 62% over 2 steps) as a clear foamy oil: R_f = 0.13 (1:9 MeOH–CH_2Cl_2); ^{1}H NMR (600 MHz, CD_3OD) δ 0.63 (dd, *J* = 8.4, 4.2 Hz, 2H), 0.87 (dd, *J* = 7.2, 4.8 Hz, 2H), 1.34 (s, 3H), 1.59 (s, 3H), 3.35–3.36 (m, 1H), 3.37–3.41 (m, 2H), 4.46 (d, *J* = 2.4 Hz, 1H), 5.09 (dd, *J* = 6.0, 2.4 Hz, 1H), 5.31 (dd, *J* = 6.0, 4.2 Hz, 1H), 6.02 (d, *J* = 4.2 Hz, 1H), 8.15 (s, 1H), 8.34 (s, 1H); ^{13}C NMR (150 MHz, CD_3OD) δ 7.7, 25.7, 27.8, 46.1, 50.0, 83.2, 84.5, 85.3, 93.1, 115.8, 121.5, 141.8, 154.1, 157.3; HRMS (ESI–) calcd for $C_{16}H_{22}N_7O_5S$ $[M – H]^-$ 424.1409, found 424.1415 (1.4 ppm error).

N^6-Cyclopropyl-5′-deoxy-5′-*N*-[*N*-(2-hydroxybenzoyl)sulfamoyl]aminoadenosine triethylammonium salt (6)

The title compound was prepared from **21** (0.20 g, 0.47 mmol) using the general procedures for salicylation and TFA deprotection. Purification by preparative reverse-phase HPLC on a Phenomenex Gemini 10 μm C18 (250 × 21.2 mm) column at a flow rate of 20 mL/min isocratic at 22% MeCN in 50 mM aqueous triethylammonium bicarbonate for 10 min, followed by washing the column with 90% MeCN for 5 min prior to re-equilibration. The retention time of the product was 7.2 minutes (k' = 1.4) and the appropriate fractions were pooled and lyophilized to afford the title compound (70.2 mg, 61%) as a white solid: ^{1}H NMR (600 MHz, CD_3OD) δ 0.63–0.66 (m, 2H), 0.87–0.90 (m, 2H), 1.12 (t, *J* = 7.8 Hz, 9H), 2.65 (s, 1H), 2.77 (q, *J* = 7.2 Hz, 6H), 3.33 (d, *J* = 4.2 Hz, 2H), 4.25 (q, *J* = 4.2 Hz, 1H), 4.37 (q, *J* = 3.0 Hz, 1H), 4.87 (solvent ovlp, 1H), 5.93 (d, *J* = 6.6 Hz, 1H), 6.75–6.79 (m, 2H), 7.26 (t, *J* = 7.8 Hz, 1H), 7.88 (d, *J* = 7.8 Hz, 1H), 8.24 (s, 1H), 8.40 (s, 1H); ^{13}C NMR (176 MHz, CD_3OD) δ 7.7, 10.5, 40.6, 46.7, 47.4, 73.2, 74.9, 86.0, 90.8, 118.0, 119.2, 121.2, 121.5, 131.0, 134.0, 141.8, 154.2, 157.3, 162.1, 174.3; HRMS (ESI–) calcd for $C_{20}H_{22}N_7O_7S$ $[M - H]^-$ 504.1307, found 504.1313 (1.1 ppm error).

5′-*N*-[*N*-(*tert*-Butoxycarbonyl)-*N*-sulfamoyl]amino-N^6-cyclopropyl-5′-deoxy-2′, 3′-*O*-isopropylidene-2-phenyladenosine (24)

The title compound was prepared from **23** (0.48 g, 1.1 mmol) using the general procedure for the Mitsunobu reaction and isolated as a foamy oil (0.868 g, 93%): R_f = 0.19 (1:1 EtOAc–hexane); ^{1}H NMR (400 MHz, $CDCl_3$) δ 0.74 (br s, 2H), 0.94 (d, *J* = 5.9 Hz, 2H), 1.28–1.25 (m, 1H), 1.41 (s, 3H), 1.48 (s, 9H), 1.62 (s, 3H), 3.22 (s, 1H), 4.02– 4.10 (m, 2H), 4.33 (q, *J* = 5.7 Hz, 1H), 5.26 (t, *J* = 5.4 Hz, 1H), 5.45 (s, 2H), 5.52 (d, *J* = 6.5 Hz, 1H), 6.12 (s, 1H), 7.44–7.52 (m, 3H), 7.89 (s, 1H), 8.42–8.46 (m, 2H); ^{13}C NMR (100 MHz, CD_3OD) δ 6.2, 24.2, 26.1, 26.7, 27.1, 48.8, 82.5, 83.5, 84.1, 85.9, 90.0, 114.1, 118.3, 127.90 (2C), 127.93, 129.7, 140.8, 151.8, 155.0, 158.8 (missing 1 aryl C); HRMS (ESI+) calcd for $C_{27}H_{35}N_7O_7SNa$ $[M + Na]^+$ 624.2211, found 624.2255 (7.1 ppm error).

N^6-Cyclopropyl-5′-deoxy-5′-*N*-[*N*-(2-hydroxybenzoyl)sulfamoyl]amino-2-phenyladenosine triethylammonium salt (7)

The title compound was prepared from **24** (0.45 g, 0.75 mmol) using the general procedure for salicylation and TFA deprotection. The crude product was purified by silica gel flash chromatography (10% MeOH–CH_2Cl_2 with 1% Et_3N) followed by preparative reverse-phase HPLC on a Phenomenex Gemini 10 μm C18 (250 × 21.2 mm) column at a flow rate of 20 mL/min with a gradient of 20–60% MeCN in 50 mM aqueous triethylammonium bicarbonate pH 7.5 over 20 min. The retention time of the product was 13.40 minutes (k' = 3.9) and the appropriate fractions were pooled and lyophilized to afford the title compound (80 mg, 18% over 2 steps) as a white solid: ^{1}H NMR (600 MHz, $CDCl_3$) δ 0.64–0.57 (m, 2H), 0.77–0.86 (m, 2H), 1.11 (t, *J* = 7.3 Hz, 9H), 2.95 (q, *J* = 7.1 Hz, 6H), 3.01 (br s, 1H), 3.33–3.44 (m, 2H), 4.32–4.38 (m, 2H), 4.56–4.60 (m, 1H), 4.72 (t, *J* = 5.1 Hz, 1H), 6.00 (d, *J* = 5.4 Hz, 1H), 6.71 (t, *J* = 7.5 Hz, 1H), 6.81 (d, *J* = 8.2 Hz, 1H), 7.22 (t, *J* = 7.2 Hz, 1H), 7.35–7.40 (m, 3H), 7.85 (d, *J* = 7.3 Hz, 1H), 8.01 (s, 1H), 8.34 (d, *J* = 7.10 Hz, 2H); ^{13}C NMR (150 MHz, $CDCl_3$) δ 7.1, 8.4, 23.8, 45.2, 46.3, 71.8, 74.9, 83.9, 88.9, 117.1, 118.1,

118.4, 119.2, 128.20, 128.22, 129.7, 129.8, 133.2, 138.3, 138.9, 149.6, 155.2, 159.0, 160.8, 173.3; HRMS (ESI–) calcd for $C_{26}H_{26}N_7O_7S$ [M – Et_3NH]$^-$ 580.1620, found 580.1589 (5.3 ppm error).

5′-*N*-[*N*-(2-Hydroxybenzoyl)sulfamoyl]amino-2′, 5′-dideoxy-2′-fluoroadenosine triethylammonium salt (8)

The title compound was prepared from **27** (0.62 g, 0.81 mmol) using the general procedure for salicylation and TFA deprotection. The crude product was purified by silica gel flash chromatography (10% MeOH–CH_2Cl_2 with 1% Et_3N) followed by preparative reverse-phase HPLC on a Phenomenex Gemini 10 μm C18 (250 × 21.2 mm) column at a flow rate of 20 mL/min with a gradient of 10–40% MeCN in 50 mM aqueous triethylammonium bicarbonate pH 7.5 over 20 min. The retention time of the product was 9.90 minutes (k' = 2.3) and the appropriate fractions were pooled and lyophilized to afford the title compound (145 mg, 38% yield over 2 steps) as a white powder: ^{1}H NMR (600 MHz, CD_3OD) δ 1.29 (t, J = 7.3 Hz, 9H), 3.14 (q, J = 7.3 Hz, 6H), 3.37–3.39 (m, 1H), 3.44 (dd, J = 13.6, 3.2 Hz, 1H), 4.25–4.29 (m, 1H), 4.66 (dt, J = 14.6, 5.3, Hz, 1H), 5.52 (dt, J = 52.6, 4.0 Hz, 1H), 6.21 (dd, J = 16.1, 3.5, 1H), 6.80 (t, J = 7.5 Hz, 1H), 6.82 (d, J = 8.2 Hz, 1H), 7.25–7.33 (m, 1H), 7.91 (dd, J = 7.9, 1.7, Hz, 1H), 8.29 (s, 1H), 8.24 (s, 1H); ^{13}C NMR (150 MHz, CD_3OD) δ 8.3, 44.3, 46.7, 70.1 (d, $^2J_{C\text{-}F}$ = 15.9 Hz), 82.6, 87.1 (d, $^2J_{C\text{-}F}$ = 33.0 Hz), 92.7 (d, $^1J_{C\text{-}F}$ = 190 Hz), 116.6, 118.1, 119.4, 129.7, 132.9, 139.9, 148.8, 152.9, 155.8, 160.2, 173.0 (missing 1 aryl C); HRMS (ESI–) calcd for $C_{17}H_{17}FN_7O_6S$ [M – Et_3NH]$^-$ 466.0951, found 466.0988 (7.9 ppm error).

3′, 5′-*O*-di-Acetyl-2′-deoxy-2′-fluoroguanosine (34)

To a stirring solution of **33** (4.00 g, 14 mmol, 1.0 equiv) in DMF (100 mL) at 23 °C were added sequentially pyridine (6.65 g, 84 mmol, 6.0 equiv) and acetic anhydride (8.6 g, 84 mmol, 6.0 equiv). The reaction mixture was stirred for 12 h at 23 °C and concentrated under reduced pressure to afford the title compound (4.1 g, 79%) as a white powder: ^{1}H NMR (400 MHz, DMSO-d_6) δ 2.03 (s, 3H), 2.14 (s, 3H), 4.22 (dd, J = 12.8, 6.4 Hz, 1H), 4.32–4.39 (m, 2H), 5.50–5.58 (m, 1H), 5.72 (ddd, J = 51.6, 5.3, 3.3 Hz, 1H), 6.11 (dd, J = 18.5, 3.2 Hz, 1H), 6.53 (s, 2H), 7.89 (s, 1H), 10.74 (s, 1H); ^{13}C NMR (100 MHz, DMSO–d_6) δ 20.3, 20.5, 62.9, 70.26 (d, $^2J_{C\text{-}F}$ = 14.5 Hz), 78.4, 85.5 (d, $^2J_{C\text{-}F}$ = 33.4 Hz), 90.8 (d, $^1J_{C\text{-}F}$ = 191 Hz), 116.8, 135.6, 150.7, 153.8, 156.6, 169.4, 170.1; HRMS (ESI+) calcd for $C_{14}H_{16}FN_5O_6Na$ [M + Na]$^+$ 392.0977, found 392.0933 (4.9 ppm error).

3′, 5′-*O*-di-Acetyl-6-chloro-2′-deoxy-2′-fluoro-2-iodoadenosine (35)

To a stirring solution of **34** (1.8 g, 4.87 mmol. 1.0 equiv) and Et_4NCl (dried in a vacuum-oven over P_2O_5) (1.62 g, 9.74 mmol, 2.0 equiv) in acetonitrile (20 mL) at 23 °C were sequentially added freshly distilled $POCl_3$ (4.48 g, 29.2 mmol, 6.0 equiv) and freshly distilled dimethylaniline (0.59 g, 4.87 mmol, 1.0 equiv). The reaction mixture was heated for 20 min at 105 °C, cooled and poured into a beaker containing ice and stirred for 30 min. The organic layer was separated and the aqueous layer was extracted with EtOAc (2 × 50 mL) and the combined organic extracts were washed with H_2O, saturated aqueous $NaHCO_3$, saturated aqueous NaCl, dried ($MgSO_4$) and concentrated under reduced pressure. The crude

product was recrystallized from isopropyl alcohol (100 mL) to afford 3′,5′-*O*-di-acetyl-6-chloro-2′-deoxy-2′-fluoroguanosine (1.77 g, 86%) as a white power that was used directly in the next step.

To a stirring solution of 3′,5′-*O*-di-acetyl-6-chloro-2′-deoxy-2′-fluoroguanosine prepared above (1.77 g, 4.56 mmol, 1.0 equiv) in THF (30 mL) at 23°C was sequentially added CH_2I_2 (12.2 g, 46 mmol, 10 equiv), I_2 (1.15 g, 4.6 mmol, 1.0 equiv), CuI (0.96 g, 5.0 mmol, 1.1 equiv) and isoamyl nitrite (1.6 g, 1.7 mmol, 3.0 equiv). The reaction mixture was then stirred at 80 °C for 1 h, cooled and concentrated under reduced pressure. Purification by flash chromatography (1:1 EtOAc–hexane) afforded the title compound (2.16 g, 95%) as a white powder: R_f = 0.45 (1:1 EtOAc–hexane); ^{1}H NMR (400 MHz, CD_3OD) δ 2.03 (s, 3H), 2.18 (s, 3H), 4.36 (dd, *J* = 12.4, 4.7 Hz, 1H), 4.45 (dd, *J* = 12.4, 3.1 Hz, 1H), 4.48–4.54 (m, 1H), 5.67 (ddd, *J* = 17.9, 7.8, 4.9 Hz, 1H), 5.81 (ddd, *J* = 51.4, 4.9, 2.0 Hz, 1H), 6.40 (dd, *J* = 18.7, 2.0 Hz, 1H), 8.58 (s, 1H); ^{13}C NMR (100 MHz, CD_3OD) δ 20.4, 20.8, 63.6, 71.6 (d, $^2J_{C\text{-}F}$ = 15.1 Hz), 80.7, 89.5 (d, $^2J_{C\text{-}F}$ = 35.2 Hz), 92.6 (d, $^1J_{C\text{-}F}$ = 192 Hz), 117.8, 133.3, 146.9, 151.1, 153.1, 171.4, 172.2; HRMS (ESI+) calcd for $C_{14}H_{13}ClFIN_4O_5Na$ $[M + Na]^+$ 520.9495, found 520.9489 (1.2 ppm error).

2′-Deoxy-2′-fluoro-2-iodoadenosine (36)

To a solution of **35** (2.0 g, 4.02 mmol, 1.0 equiv) in MeOH (5 mL) in a high-pressure tube was added a 7 N ammonia solution in methanol (20 mL, 140 mmol, 35 equiv). The vessel was sealed and heated at 70 °C for 16 h. After cooling to rt, the reaction mixture was purged with N_2 for 1 h to remove ammonia and then concentrated under reduced pressure to afford the title compound (1.20 g, 56%) as a white powder contaminated with 2.3 equiv of acetamide (the calculated yield takes into account the acetamide): R_f = 0.18 (EtOAc); ^{1}H NMR (400 MHz, CD_3OD) δ 3.79 (dd, *J* = 12.5, 3.7 Hz, 1H), 3.94 (dd, *J* = 12.6, 2.4 Hz, 1H), 4.11–4.16 (m, 1H), 4.62 (ddd, *J* = 16.5, 6.4, 4.5 Hz, 1H), 5.39 (ddd, *J* = 52.7, 4.5, 2.9 Hz, 1H), 6.23 (dd, *J* = 16.3, 2.9 Hz, 1H), 8.26 (s, 1H); ^{13}C NMR (100 MHz, CD_3OD) δ 62.7, 70.4 (d, $^2J_{C\text{-}F}$ = 16.1 Hz), 85.9, 88.5 (d, $^2J_{C\text{-}F}$ = 33.3 Hz), 94.9 (d, $^1J_{C\text{-}F}$ = 188 Hz), 120.5, 120.8, 141.2, 150.5, 157.2; HRMS (ESI+) calcd for $C_{10}H_{12}FIN_5O_3$ $[M + H]^+$ 395.9963, found 395.9964 (0.3 ppm error).

3′, 5′-*O*-bis(*tert*-Butyldimethylsilyl)-2′-deoxy-2′-fluoro-2-iodoadenosine (37)

To a stirring solution of **36** (1.90 g, 4.8 mmol, 1.0 equiv) in DMF (20 mL) at 0 °C was sequentially added TBSCl (2.17 g, 14.4 mmol, 3.0 equiv), imidazole (1.64 g, 24 mmol, 5 equiv) and DMAP (59 mg, 0.48 mmol, 0.1 equiv). The reaction mixture was stirred at 23 °C for 24 h and concentrated under reduced pressure. Purification by flash chromatography (1:1 EtOAc–hexane) afforded the title compound (2.97 g, 97%) as a yellow oil: R_f = 0.5 (1:1 EtOAc–hexane); ^{1}H NMR (400 MHz, CD_3OD) δ –0.09 (s, 3H), 0.01 (s, 3H), 0.24 (s, 6H), 0.79 (s, 9H), 0.96 (s, 9H), 3.79 (dd, *J* = 11.7, 2.9 Hz, 1H), 3.94–4.05 (m, 2H), 4.97 (ddd, *J* = 20.8, 7.6, 4.3 Hz, 1H), 5.59 (ddd, *J* = 53.2, 4.4, 1.5 Hz, 1H), 6.15 (dd, *J* = 19.8, 1.5 Hz, 1H), 8.13 (s, 1H); ^{13}C NMR (100 MHz, CD_3OD) δ –5.2, –5.1, –4.4, –4.0, 19.1, 19.3, 26.38, 26.47, 62.8, 70.7 (d, $^2J_{C\text{-}F}$ = 15.9 Hz), 84.9, 89.2 (d, $^2J_{C\text{-}F}$ = 34.6 Hz), 94.1 (d, $^1J_{C\text{-}F}$ = 188 Hz), 120.5, 121.0, 141.9, 150.5, 157.2; HRMS (ESI+) calcd for $C_{22}H_{39}FIN_5O_3Si_2Na$ $[M + Na]^+$ 646.1512, found 646.1540 (4.3 ppm error).

3′, 5′-*O-tert*-Butyldimethylsilyl-2′-deoxy-2′-fluoro-2-phenyladenosine (38)

To a stirring solution of **37** (1.1 g, 1.76 mmol, 1.0 equiv) in dioxane (10 mL) at 23 °C was sequentially added phenylboronic acid (0.65 g, 5.3 mmol, 3.0 equiv), K_3PO_4 (1.12 g, 5.3 mmol, 3.0 equiv), $Pd(OAc)_2$ (0.119 g, 0.53 mmol, 0.3 equiv) and CyJohnPhos (0.185 g, 0.53 mmol, 0.3 equiv). The reaction mixture was purged with argon for 15 min, sealed and heated at 100 °C for 12 h. The reaction was cooled to 23 °C, filtered through a pad of Celite and concentrated under reduced pressure. Purification by flash chromatography (1:1 EtOAc–hexane) afforded the title compound (0.68 g, 67%) as a yellow solid: R_f = 0.5 (1:1 EtOAc–hexane): ^{1}H NMR (400 MHz, CD_3OD) δ –0.09 (s, 3H), –0.02 (s, 3H), 0.17 (s, 6H), 0.77 (s, 9H), 0.95 (s, 9H), 3.83 (dd, *J* = 11.6, 2.9 Hz, 1H), 3.99–4.08 (m, 2H), 4.96 (ddd, *J* = 19.2, 7.2, 4.5 Hz, 1H), 5.71 (ddd, *J* = 53.4, 4.6, 1.9 Hz, 1H), 6.27 (dd, *J* = 19.4, 1.9 Hz, 1H), 7.39–7.44 (m, 3H), 8.24 (s, 1H), 8.30–8.36 (m, 2H); ^{13}C NMR (100 MHz, CD_3OD) δ –5.24, –5.22, –4.5, –4.2, 19.0, 19.3, 26.29, 26.43, 62.4, 70.7 (d, $^2J_{C\text{-}F}$ = 15.9 Hz), 85.1, 89.4 (d, $^2J_{C\text{-}F}$ = 34.3 Hz), 93.9 (d, $^1J_{C\text{-}F}$ = 189 Hz), 119.4, 129.2, 129.5, 131.0, 139.8, 142.0, 151.5, 157.3, 161.3; HRMS (ESI+) calcd for $C_{28}H_{44}FN_5O_3Si_2Na$ $[M + Na]^+$ 596.2859, found 596.2853 (1.0 ppm error).

3′-*O-tert*-Butyldimethylsilyl-2′-deoxy-2′-fluoro-2-phenyladenosine (39)

To a stirring solution AcOH–THF–H_2O (9:1:1, 10 mL) at 0 °C was added **38** (0.674 g, 1.17 mmol, 1.0 equiv). The reaction mixture was warmed to 23 °C and stirred for 24 h and concentrated. Purification by flash chromatography (3:1 EtOAc–hexane) afforded the title compound (0.378 g, 70%) as a white solid. R_f = 0.28 (3:1 EtOAc–hexane): ^{1}H NMR (400 MHz, CD_3OD) δ 0.17 (s, 3H), 0.20 (s, 3H), 0.97 (s, 9H), 3.75 (dd, *J* = 12.4, 4.0, 1H), 3.94 (dd, *J* = 12.4, 2.7 Hz, 1H), 4.10–4.14 (m, 1H), 4.91–4.99 (m, 1H), 5.61 (ddd, *J* = 52.2, 4.8, 2.9, Hz, 1H), 6.32 (dd, *J* = 18.1, 2.9 Hz, 1H), 7.42–7.46 (m, 3H), 8.31–8.37 (m, 3H); ^{13}C NMR (100 MHz, CD_3OD) δ –4.7, –4.5, 19.1, 26.3, 62.0, δ 71.8 (d, $^2J_{C\text{-}F}$ = 15.5 Hz,), 86.2, 89.1 (d, $^2J_{C\text{-}F}$ = 33.8 Hz), 94.1 (d, $^1J_{C\text{-}F}$ = 191 Hz), 119.6, 129.3, 129.5, 131.0, 139.9, 142.1, 151.6, 157.4, 161.4; HRMS (ESI+) calcd for $C_{22}H_{30}FN_5O_3SiNa$ $[M + Na]^+$ 482.1994, found 482.2123 (26 ppm error).

5′-Azido-3′-*O-tert*-butyldimethylsilyl-2′-deoxy-2′-fluoro-2-phenyladenosine (40)

To a stirring solution of **39** (0.268 g, 0.58 mmol, 1.0 equiv) in dioxane (5.0 mL) at 23 °C were added sequentially DPPA (0.376 mL, 1.74 mmol, 3.0 equiv) and DBU (0.175 mL, 1.16 mmol, 2.0 equiv). The reaction mixture was stirred for 12 h at 23 °C then NaN_3 (0.38 g, 5.8 mmol, 10 equiv) and 15-crown-5 (13 mg, 0.060 mmol, 0.1 equiv) were added and the reaction was heated at 90 °C for another 12 h. The reaction was then cooled and concentrated under reduced pressure. Purification by flash chromatography (3:1 EtOAc–hexane) afforded the title compound (0.240 g, 85%) as a white powder: R_f = 0.56 (3:1 EtOAc–hexane); ^{1}H NMR (400 MHz, CD_3OD) δ 0.16 (s, 3H), 0.22 (s, 3H), 0.95 (s, 9H), 3.41 (dd, *J* = 13.7, 3.9 Hz, 1H), 3.80 (dd, *J* = 13.8, 3.0, Hz, 1H), 4.15–4.21 (m, 1H), 5.33 (ddd, *J* = 19.1, 7.9, 5.0 Hz, 1H), 5.64 (ddd, *J* = 53.6, 5.0. 1.7 Hz, 1H), 6.27 (dd, *J* = 21.9, 1.7 Hz, 1H), 7.42–7.47 (m, 3H), 8.22 (s, 1H), 8.38–8.43 (m, 2H); ^{13}C NMR (100 MHz, CD_3OD) δ –4.6, –4.4, 19.0, 26.2, 51.4, 71.9 (d, $^2J_{C\text{-}F}$ = 16.1 Hz), 83.6, 89.8 (d, $^2J_{C\text{-}F}$ = 35.7 Hz), 94.2 (d, $^1J_{C\text{-}F}$ = 189 Hz), 119.7, 129.3, 129.4, 131.0, 139.9, 142.5, 151.5, 157.4, 161.4;

HRMS (ESI+) calcd for $C_{22}H_{29}FN_8O_2SiNa$ $[M + Na]^+$ 507.2059, found 507.2025 (6.7 ppm error).

2′, 5′-Dideoxy-2′-fluoro-5′-[*N*-(sulfamoyl)amino]-2-phenyladenosine (41)

To a round-bottomed flask containing **40** (0.230 g, 0.47 mmol, 1.0 equiv) purged with argon was added anhydrous MeOH (5.0 mL) followed by Pd/C (0.100 g, 10% by weight) and the flask evacuated by house vacuum and back-filled with a H_2 balloon 3 times before being allowed to stir vigorously under a H_2 balloon at 23 °C for 1 h. The crude reaction mixture was filtered over a pad of Celite and concentrated under reduced pressure to afford crude the amine, which was then dissolved in dioxane (6 mL). Sulfamide (0.136 g, 1.5 mmol, 3.0 equiv) was added and the reaction mixture was then heated at 90 °C for 3 h. The reaction was cooled, concentrated under reduced pressure and purified by flash chromatography (3:1 EtOAc–hexane) to afford the title compound (0.190 g, 87% over 2 steps) as a white powder: R_f = 0.3 (3:1 EtOAc–hexane); ^{1}H NMR (400 MHz, CD_3OD) δ 0.17 (s, 3H), 0.23 (s, 3H), 0.97 (s, 9H), 3.33–3.39 (m, 1H), 3.53 (dd, *J* = 13.6, 3.8 Hz, 1H), 4.18–4.24 (m, 1H), 5.04 (ddd, *J* = 15.9, 6.8, 4.9 Hz, 1H), 5.66 (ddd, *J* = 53.2, 5.0, 2.7 Hz, 1H), 6.28 (dd, *J* = 19.6, 2.7 Hz, 1H), 7.41–7.46 (m, 3H), 8.24 (s, 1H), 8.32– 8.38 (m, 2H); ^{13}C NMR (100 MHz, CD_3OD) δ –4.5, –4.4, 19.1, 26.3, 45.5, 72.7 (d, $^2J_{C\text{-}F}$ = 15.8 Hz), 83.8, 89.2 (d, $^2J_{C\text{-}F}$ = 34.5 Hz), 93.8 (d, $^1J_{C\text{-}F}$ = 191 Hz), 119.6, 129.4, 129.5, 131.0, 139.8, 142.4, 151.6, 157.4, 161.5; HRMS (ESI+) calcd for $C_{22}H_{32}FN_7O_4SSiNa$ $[M + Na]^+$ 560.1882, found 560.1890 (1.4 ppm error).

2′, 5′-Dideoxy-2′-fluoro-5′-*N*-[*N*-(2-hydroxybenzoyl)sulfamoyl]amino-2-phenyladenosine triethylammonium salt (9)

The title compound was prepared from **41** (0.176 g, 0.33 mmol, 1.0 equiv) using the general procedure for salicylation and TFA deprotection. The crude product was purified by silica gel flash chromatography (10% MeOH–CH_2Cl_2 with 1% Et_3N) followed by preparative reverse-phase HPLC on a Phenomenex Gemini 10 μm C18 (250 × 21.2 mm) column at a flow rate of 25 mL/min with 30% MeCN in 50 mM aqueous triethylammonium bicarbonate pH 7.5 over 20 min. The retention time of the product was 12.0 minutes (k' = 3.1) and the appropriate fractions were pooled and lyophilized to afford the title compound (95 mg, 45% over 2 steps) as a white powder: ^{1}H NMR (400 MHz, CD_3OD) δ 1.21 (t, *J* = 7.3 Hz, 14H, excess Et_3N), 2.98 (q, *J* = 7.3 Hz, 10H, excess Et_3N), 3.35–3.30 (ovlp m, 1H), 3.47 (dd, *J* = 13.5, 3.5 Hz, 1H), 4.19–4.25 (m, 1H), 4.80–4.86 (ovlp m, 1H), 5.57 (ddd, *J* = 53.2, 4.9, 2.2 Hz, 1H), 6.28 (dd, *J* = 19.1, 2.1 Hz, 1H), 6.71–6.78 (m, 2H), 7.22–7.27 (m, 1H), 7.37–7.45 (m, 3H), 7.83 (dd, *J* = 7.8, 1.7 Hz, 1H), 8.27 (s, 1H), 8.31–8.37 (m, 2H); ^{13}C NMR (100 MHz, CD_3OD) δ 9.9, 46.0, 47.7, 71.8 (d, $^2J_{C\text{-}F}$ = 16.2 Hz), 82.9, 88.6 (d, $^2J_{C\text{-}F}$ = 34.3 Hz), 95.0 (d, $^1J_{C\text{-}F}$ = 187 Hz), 117.9, 119.2, 121.0, 129.32, 129.37, 129.39, 130.94, 130.97, 134.0, 139.7, 141.7, 151.6, 157.3, 161.3, 161.9, 174.6; HRMS (ESI+) calcd for $C_{23}H_{22}FN_7O_6SNa$ $[M – Et_3N + Na]^+$ 566.1229, found 566.1250 (3.7 ppm error).

5′-*O*-*tert*-Butyldimethylsilyl-2′-deoxy-2′-fluoroadenosine (43).[50]

To a stirring solution of **42** (0.750 g, 2.8 mmol, 1.0 equiv) in DMF (25 mL) at 0 °C was added sequentially TBSCl (0.462 g, 4.5 mmol, 1.6 equiv) and imidazole (0.322 g, 4.7 mmol,

1.7 equiv). The reaction mixture was stirred for 7 h at 23 °C, then quenched with MeOH (20 mL) and concentrated. Purification by flash chromatography (4:1 EtOAc–hexane) afforded the title compound (0.79 g, 90%) as a white solid. The analytical data (^{1}H NMR, ^{19}F NMR, MS) agreed with previously reported values.[50] ^{13}C NMR data and R_f have not been disclosed and are provided herein: R_f = 0.22 (EtOAc); ^{13}C NMR (100 MHz, CD_3OD) δ –5.25, –5.22, 19.4, 26.5, 62.5, 69.4 (d, $^2J_{C\text{-}F}$ = 16.6 Hz), 84.5, 88.2 (d, $^2J_{C\text{-}F}$ = 33.6 Hz), 95.3 (d, $^1J_{C\text{-}F}$ = 187 Hz), 120.4, 140.8, 150.0, 154.1, 157.3.

5′-*O*-*tert*-Butyldimethylsilyl-2′-deoxy-2′-fluoro-3′-*O*-(phenoxythiocarbonyl)adenosine (44).[50]

To a stirring solution of **43** (0.800 g, 2.1 mmol, 1.0 equiv) in MeCN (25 mL) was added sequentially *O*-phenyl chlorothionoformate (0.540 g, 3.1 mmol, 1.5 equiv) and DMAP (0.765 g, 6.3 mmol, 3.0 equiv). The reaction mixture was stirred for 1 h at 23 °C then quenched with H_2O (10 mL). The aqueous layer was extracted with EtOAc (2 × 20 mL) and the combined organic layers were washed with saturated aqueous NaCl, dried ($MgSO_4$), filtered and concentrated under reduced pressure. Purification by flash chromatography (4:1 EtOAc–hexane) afforded the title compound (0.79 g, 82%) as an orange solid. The analytical data (^{1}H NMR, ^{19}F NMR, MS) agreed with previously reported values.[50] ^{13}C NMR data and R_f have not been disclosed and are provided herein: R_f = 0.38 (3:1 EtOAc–hexane); ^{13}C NMR (100 MHz, $CDCl_3$) δ –5.5, –5.4, 18.4, 25.9, 61.8, 77.6 (d, $^2J_{C\text{-}F}$ = 14.0 Hz), 81.6, 86.3 (d, $^2J_{C\text{-}F}$ = 32.1 Hz), 90.7 (d, $^1J_{C\text{-}F}$ = 196.8 Hz), 119.9, 121.6, 126.9, 129.7, 138.5, 149.6, 153.38, 153.42, 155.6, 193.9.

2′, 3′-Dideoxy-2′-fluoroadenosine (46).[50]

To a stirring solution of **44** (0.410 g, 0.80 mmol) in toluene (10 mL) was added sequentially AIBN (0.026 g, 0.16 mmol, 0.2 equiv) and Bu_3SnH (0.425 mL, 1.6 mmol, 2.0 equiv). The reaction mixture was degassed with Ar for 30 min then heated at 85 °C for 3 h. Upon completion, the reaction mixture was cooled, concentrated and filtered through a plug of silica gel, washing with EtOAc, to obtain **45** (0.235 g, 79% crude yield) as a yellow solid that was used directly in the next step.

To a stirring solution of **45** (0.210 g, 0.57 mmol, 1.0 equiv) in MeOH (5 mL) at 0 °C was added TFA (5 mL). The reaction mixture was stirred for 12 h at 0 °C and concentrated under reduced pressure. Purification by flash chromatography (1:19 MeOH–EtOAc) afforded the title compound (0.132 g, 92%) as a white powder: R_f = 0.18 (1:19 MeOH–EtOAc); ^{1}H NMR (400 MHz, DMSO-d_6) δ 2.23 (ddd, *J* = 20.6, 14.5, 5.5 Hz, 1H), 2.35–2.55 (m, 1H), 3.55 (ddd, *J* = 12.1, 5.5, 3.9 Hz, 1H), 3.74 (ddd, *J* = 12.1, 5.3, 3.0 Hz, 1H), 4.28–4.50 (m, 1H), 5.14 (t, *J* = 5.5 Hz, 1H), 5.59 (dd, *J* = 51.9, 4.3, Hz, 1H), 6.23 (d, *J* = 18.3 Hz, 1H), 7.30 (s, 2H), 8.14 (s, 1H), 8.34 (s, 1H); ^{13}C NMR (100 MHz, DMSO-d_6) δ 32.3 (d, $^2J_{C\text{-}F}$ = 20.3 Hz), 62.0, 81.8, 88.9 (d, $^2J_{C\text{-}F}$ = 35.8 Hz), 97.3 (d, $^1J_{C\text{-}F}$ = 177.4 Hz), 119.4, 139.2, 149.1, 153.1, 156.5; HRMS (ESI+) calcd for $C_{10}H_{12}FN_5O_2Na$ $[M + Na]^+$ 276.0867, found 276.0860 (2.5 ppm error).

5′-Azido-2′, 3′, 5′-trideoxy-2′-fluoroadenosine (47)

To a stirring solution of **46** (0.20 g, 0.87 mmol, 1.0 equiv) in dioxane (5.0 mL) at 23 °C was added sequentially DPPA (0.56 mL, 2.6 mmol, 3.0 equiv) and DBU (0.39 mL, 2.6 mmol, 3.0 equiv). The reaction mixture was stirred for 12 h at 23 °C then NaN_3 (0.55 g, 8.6 mmol, 10 equiv) and 15-crown-5 (0.035 mL, 0.17 mmol, 0.2 equiv) were added and the reaction was heated at 90 °C for another 12 h. The reaction was then cooled and concentrated under reduced pressure. Purification by flash chromatography (EtOAc) afforded the title compound (0.145 g, 66%) as a white powder: R_f = 0.33 (EtOAc); ^{1}H NMR (400 MHz, CD_3OD) δ 2.38 (ddd, *J* = 20.4, 14.5, 5.4 Hz, 1H), 2.67 (dddd, *J* = 41.1, 15.0, 10.6, 4.7 Hz, 1H), 3.53 (dd, *J* = 13.4, 4.8, Hz, 1H), 3.72 (dd, *J* = 13.4, 3.3 Hz, 1H), 4.56–4.66 (m, 1H), 5.71 (dd, *J* = 51.6, 4.7, Hz, 1H), 6.31 (d, *J* = 19.3 Hz, 1H), 8.21 (s, 1H), 8.26 (s, 1H); ^{13}C NMR (100 MHz, CD_3OD) 35.1 (d, $^2J_{C\text{-}F}$ = 21.0 Hz), 54.1, 81.2, 91.2 (d, $^2J_{C\text{-}F}$ = 37.3 Hz, H), 97.9 (d, $^1J_{C\text{-}F}$ = 180 Hz), 120.5, 140.9, 150.3, 154.1, 157.5; HRMS (ESI+) calcd for $C_{10}H_{11}FN_8ONa$ $[M + Na]^+$ 301.0932, found 301.0951 (6.3 ppm error).

2′, 3′, 5′-Trideoxy-2′-fluoro-5′-[*N*-(sulfamoyl)amino]adenosine (48)

To a round-bottomed flask containing **47** (0.145 g, 0.5 mmol, 1.0 equiv) purged with argon was added MeOH (4.0 mL) followed by Pd/C (0.055 g, 10% by weight) and the flask evacuated by house vacuum and backfilled with a H_2 balloon 3 times before being allowed to stir vigorously under a H_2 balloon at 23 °C for 1 h. The crude reaction mixture was filtered over a pad of Celite and concentrated under reduced pressure to afford crude amine, which was then dissolved in dioxane (4 mL). Sulfamide (0.145 g, 1.5 mmol, 3.0 equiv) was added and the reaction mixture was then heated at 90 °C for 3 h. The reaction was cooled, concentrated under reduced pressure and purified by flash chromatography (EtOAc) to afford the title compound (0.114 g, 60% over 2 steps) as a white powder: R_f = 0.21 (EtOAc); ^{1}H NMR (400 MHz, CD_3OD) δ 2.38 (dddd, *J* = 22.0, 14.5, 5.9, 1.8 Hz, 1H), 2.65 (dddd, *J* = 37.0, 14.9, 9.9, 5.3 Hz, 1H), 3.32 (ovlp dd, *J* = 13.8, 3.7 Hz, 1H), 3.45 (dd, *J* = 13.8, 3.7 Hz, 1H), 4.58–4.66 (m, 1H), 5.59 (dd, *J* = 52.3, 3.8, Hz, 1H), 6.23 (d, *J* = 18.8 Hz, 1H), 8.21 (s, 1H), 8.23 (s, 1H); ^{13}C NMR (100 MHz, CD_3OD) δ 33.6 (d, $^2J_{C\text{-}F}$ = 20.8 Hz), 45.2, 79.3, 90.2 (d, $^2J_{C\text{-}F}$ = 36.7 Hz, H), 96.2 (d, $^1J_{C\text{-}F}$ = 181 Hz), 119.2, 139.8, 148.5, 152.6, 155.9; HRMS (ESI+) calcd for $C_{10}H_{14}FN_7O_3SNa$ $[M + Na]^+$ 354.0755, found 354.0772 (4.8 ppm error).

2′, 3′, 5′-Trideoxy-5′-*N*-[*N*-(2-hydroxybenzoyl)sulfamoyl]amino-2′-fluoroadenosine triethylammonium salt (10)

The title compound was prepared from **48** (0.075 g, 0.23 mmol, 1.0 equiv) using the general procedure for salicylation and TFA deprotection. The crude product was purified by silica gel flash chromatography (1:9 MeOH–CH_2Cl_2 with 1% Et_3N) followed by preparative reverse-phase HPLC on a Phenomenex Gemini 10 μm C18 (250 × 21.2 mm) column at a flow rate of 25 mL/min with 25% MeCN in 50 mM aqueous triethylammonium bicarbonate pH 7.5 over 20 min. The retention time of the product was 13.3 minutes (k' = 3.5) and the appropriate fractions were pooled and lyophilized to afford the title compound (0.044 g, 34% yield over 2 steps) as a white powder: ^{1}H NMR (400 MHz, CD_3OD) δ 1.22 (t, *J* = 7.3 Hz, 9H), 2.30–2.47 (m, 1H), 2.59 (dddd, *J* = 39.0, 14.9, 10.2, 5.0 Hz, 1H), 2.99 (q, *J* = 7.2

Hz, 6H), 3.26 (dd, *J* = 13.6, 5.5 Hz, 1H), 3.39 (dd, *J* = 13.5, 3.8 Hz, 1H), 4.57–4.65 (m, 1H), 5.60 (dd, *J* = 52.1, 4.8 Hz, 1H), 6.24 (d, *J* = 18.3 Hz, 1H), 6.74–6.80 (m, 2H), 7.24–7.29 (m, 1H), 7.87 (dd, *J* = 7.8, 1.8 Hz, 1H), 8.21 (s, 1H), 8.31 (s, 1H); ^{13}C NMR (100 MHz, CD_3OD) δ 9.4, 35.3 (d, $^2J_{C\text{-}F}$ = 20.6 Hz) 47.4, 48.0, 81.1, 91.3 (d, $^2J_{C\text{-}F}$ = 36.7 Hz), 97.9 (d, $^1J_{C\text{-}F}$ = 180 Hz), 117.9, 119.2, 121.0, 131.0, 134.1, 141.0, 150.2, 154.1, 157.4, 162.0, 174.4 (missing 1 aryl C); HRMS (ESI–) calcd for $C_{17}H_{17}FN_7O_5S$ $[M - Et_3NH]^-$ 450.1001, found 450.1007 (1.3 ppm error).

MbtA Enzyme Assay

MbtA was expressed in *E. coli* and purified as described.[32] MbtA concentration was determined by active site titration with **1** as described.[32] The inhibition assays were performed as reported in duplicate under initial velocity conditions.[32] In brief, the reaction was initiated by adding 10 μL [^{32}P]PP_i with 7 nM MbtA in 90 μL reaction buffer (278 μM salicylic acid, 11.1 mM ATP, 1.11 mM PPi, 83.3 mM Tris-HCl, pH 7.5, 11.1 mM $MgCl_2$, 2.22 mM DTT) at 37 °C in the presence of eight different concentrations of the inhibitor (1.5-fold dilution from 100 nM down to 5.85 nM). The reaction was terminated at 20 min by the addition of 200 μL of quenching buffer (350 mM $HClO_4$, 100 mM PPi, 1.8% *w/v* activated charcoal). The charcoal was pelleted by centrifugation and washed once with 500 μL H_2O and analyzed by liquid scintillation counting as described. Fractional initial velocities were fit by nonlinear regression analysis to the Morrison equation[60] (eq 1) using GraphPad Prism 5.0:

$$\frac{v_i}{v_0} = 1 - \frac{([E]+[I]+K_i^{app}) - \sqrt{([E]+[I]+K_i^{app})^2 - 4[E][I]}}{2[E]} \quad (1)$$

where *I* represents the concentration of inhibitor, K_i^{app} is the apparent inhibition constant, *E* is the active enzyme concentration (determined by active-site titration), v_i is the initial rate at each [*I*], and v_0 is the initial rate of the DMSO control.

M. tuberculosis H37Rv MIC Assay

All compounds minimum inhibitory concentrations (MICs) were experimentally determined as previously described.[28] MICs were determined in triplicate in iron-deficient GAST according to the broth microdilution method using compounds from DMSO stock solutions or with control wells treated with an equivalent amount of DMSO. Isoniazid was used as a positive control while DMSO was employed as a negative control. All measurements reported herein used an initial cell density of 10^4–10^5 cells/assay and growth monitored at 10–14 days, with the untreated and DMSO-treated control cultures reaching an OD_{620} 0.2–0.3. Plates were incubated at 37 °C (100 μL/well) and growth was recorded by measurement of optical density at 620 nm.

Procedures for the measurement of the oral bioavailability in Sprague-Dawley rats

Sample Collection—Sprague-Dawley rats (female, 250–274 g, Harlan Laboratories, Inc. Indianapolis, IN) were obtained with surgically implanted in-dwelling dual jugular vein/femoral vein catheters for compound infusion and blood withdrawal, respectively. Catheters

were maintained by following the Harlan Surgically Modified Animal Models: Catheter Maintenance Recommendations provided by Harlan Laboratories. All animal care, housing, and laboratory procedures were approved by the University of Minnesota Institutional Animal Care and Use Committee (IACUC) prior to these investigations (IACUC #1208A18543). The animal care and housing was maintained by University of Minnesota Research Animal Resources (RAR) and veterinarian staff. Rats were allowed to acclimate for 7 d prior to participation in a study to ensure proper patency of the catheter lines as well as to observe that there were no adverse effects on the animals due to surgery or shipping. Oral doses of investigational compounds (25 mg/kg) were suspended in either 0.5% sodium carboxymethylcelluose (Aldrich, St. Louis, MO; for compounds **1, 3**–**6, 8**–**10**) or dissolved in 25% wt/vol hydroxypropyl-β-cyclodextrin (Cargill, Inc. Cedar Rapids, IA; for compounds **2, 3**) or in 50% PEG and 5% tween 80 (for compound **7**) in sterile water as solubility allowed. Animals (3 per compound) were initially dosed via oral gavage with a ball-tipped feeding needle inserted through the mouth and esophagus with a 10 mg/mL solution of compound. The rats were restrained by holding them with 2 fingers over their shoulders with the thumb wrapped around underneath their shoulders to tilt their head up, and solution dispensed over 15–20 seconds. Rats were returned to their cages after drug administration with access to food and water *ad libitum*, and blood was removed in 0.25 mL aliquots from the left femoral vein catheter via tuberculin syringe with a sterile 22 gauge blunted needle (SAI Infusions, Inc. Lake Villa, IL) at the following time points: 0, 15, 30, 45, 60, 120, 240, and 480 min. Blood was immediately injected into a 2 mL vacutainer (Becton Dickinson, Franklin Lakes, NJ) containing 3.6 mg K_2EDTA. Subsequently, blood was centrifuged at 2,000 × *g* to separate the plasma from the hematocrit. Plasma was separated into two 50 μL aliquots that were immediately chilled on ice and transferred to −80 °C within 2 h.

Rats were given a 3-day period to wash any remaining compound from their system. Intravenous doses of investigational compounds (2.5 mg/kg) were prepared in either 0.05% sodium carboxymethylcellulose (Aldrich, St. Louis, MO; for compounds **1, 3**–**6, 8**–**10**) or 25% wt/vol hydroxypropyl-β-cyclodextrin (Cargill, Inc. Cedar Rapids, IA; for compoounds **2, 3, 7**) in sterile water as solubility allowed. The same triplicate set was then dosed via infusion in the right jugular vein catheter over 5 sec via a tuberculin syringe with a sterile 22 gauge blunted needle. Rats were returned to their cages after drug administration with access to food and water *ad libitum*, and 0.25 mL aliquots of blood were removed from the left femoral vein catheter via tuberculin syringe with a sterile 22 gauge blunted needle at the following time points: 0, 5, 10, 15, 30, 45, 60, 120, 240, and 480 min. The blood was processed in an identical manner as described for the oral dosing above.

Plasma Sample Preparation—For compounds **1**–**6**, sample plasma (20 μL) was protein-precipitated with cold acetonitrile (MeCN, 200 μL) containing N^6-cyclopropyl-2-phenyl-5′-*O*-[*N*-(salicyl)sulfamoyl]adenosine (CCA-086)[35] as the internal standard (IS) at a final concentration of 100 nM in MeCN. For compounds **7**–**10**, sample plasma (20 μL) was protein precipitated with ice-cold 10% aqueous trichloroacetic acid solution (200 μL) containing the indicated internal standard at 100 nM (**7**: IS=**1; 8**: IS=CCA-086; **9**: IS=**8; 10**: IS=**8**). For INH analysis, nicotinamide (500 nM) was used as the internal standard. The high concentrations for the IV samples of compounds **8–10** required dilution to fit within the

standard curve. This was done using rat plasma in K_2EDTA (BioChemed, Winchester, VA) from pooled female Sprague-Dawley rats. Samples from 5, 10, 15, and 30 min time points were diluted 10-fold, while the 60, and 120 min time point samples were diluted 5-fold. In the final analysis the concentrations were adjusted accordingly. After adding either the MeCN or 10% TCA solution containing internal standard, samples were vortexed for 5 sec, centrifuged at 14,000 × g for 1 min at 4 °C, and the supernatant was analyzed via LC–MS/MS. Standards were prepared in pooled female Sprague-Dawley rat plasma in K_2EDTA (BioChemed, Winchester, VA) and processed in a similar fashion as animal plasma samples.

Instrumentation—LC-MS/MS analysis was performed using an Agilent (Santa Clara, CA) 1260 Infinity gradient solvent delivery system, an Agilent 1260 Infinity HiP ALS autosampler, an Agilent 1260 column oven; or by a Shimadzu UFLC XR, SIL-20AC autosampler, and prominence CTO-20A column oven with an AB SCIEX QTRAP 5500 (Framingham, MA) mass spectrometer fitted with an electrospray ionization source. The instruments were run using Analyst Software (version 1.5.2, AB SCIEX).

Chromatography—Reverse-phase HPLC analysis was performed by gradient HPLC on a Kinetix C18 column (50 mm × 2.1 mm, 2.6 μm particle size; Phenomenex, Torrance, CA) for **1– 10** and a Synergy Hydro RP (250 mm × 2.0 mm, 4 μm particle size; Phenomenex, Torrance, CA) for isoniazid. Mobile phase A was 0.1% aqueous formic acid while mobile phase B was 0.1% formic acid in acetonitrile. Initial conditions were 5% B from 0 to 0.5 min, after which the %B was increased to 95% from 0.5 to 1 min. The column was washed in 95% B for 3 min, returned to 5% over 0.2 min, and allowed to re-equilibrate for 3.8 min in 5% B to provide a total run time of 8 min. The flow rate was 0.5 mL/min and the column oven was maintained at 40 °C. The injection volume was 10 μL.

Mass spectrometry—All analytes were analyzed in positive ionization mode by Multiple Reaction Monitoring (MRM) with the following mass spectrometry settings: entrance potential = 10 V; curtain gas = 40 psi; collision gas = medium; ionspray voltage = 5500 V; temperature = 600 °C; ion source gas 1 = 45 psi; ion source gas 2 = 40 psi. Nitrogen was used for the nebuliser and collision gas. To determine the optimum MRM settings (Table 4), each analyte was infused at a concentration of 10 μM (in 1:1 water:acetonitrile containing 0.1% formic acid) onto the MS by a syringe pump at a flow of 10 μL/min.

Data Analysis—Analyte and internal standard peak areas were calculated with MultiQuant Software (version 2.0.2, AB SCIEX, Framingham, MA). Analyte peak areas were normalized to internal standard peak areas, and the concentrations of the compounds as a triethylamine salt were calculated with the appropriate standard curve. Standard curves displayed good linearity with $R^2 = 0.99$. Pharmacokinetic parameters were calculated from concentration-time profiles by non-compartmental analysis using Phoenix WinNonLin (version 6.3, Pharsight). Linear trapezoidal linear interpolation was used to fit the data points and all the pharmacokinetic parameters were determined using the software. Bioavailability was calculated individually for each rat from the oral and intravenous data.

Caco-2 Studies

Studies to detemine permeability in Caco-2 monolayers followed the protocol described by Hubatsch and co-workers.[61]

Cultivation of Caco-2 cells on Transwell permeable supports—Caco-2 cells (ATCC® HTB-37™) of passage number (50–70) were used for studies of all compounds. Caco-2 cells from the stock were thawed and cultivated to the required passage number and cells were seeded on the filter support. Cells were grown using Dulbecco's modified Eagle's medium (DMEM) media containing 17% fetal calf serum and 1% PEST (penicillin 10,000 U mL^{-1}, streptomycin 10,000 μg mL^{-1}). Cells of required passage number were then transferred to the 12-well, 12 mm insert, 0.4 μm pore size Transwell membrane plate (Corning No. 3401) and were grown in the plates for 21 days (37 °C, CO_2 incubator, 5% CO_2, water saturated atmosphere). The media was changed every two days to support the required amount of growth.

Experimental method—The media in the plates was aspirated and the apical side washed twice with cell assay buffer (CAB) pH 6.0 (NaCl 3.56 g, $NaHCO_3$ 1.05 g, glucose 0.9 g, MES 0.975 g, KCl 0.112 g, $MgSO_4$ 0.147 g, $CaCl_2$ 0.10 g, K_2HPO_4 0.035 g in 500 mL of water). The basolateral side was washed with CAB pH 7.4 (Same composition as CAB 6.0, except HEPES 1.19 g for MES). The apical side was filled with 0.5 mL of CAB pH 6.0 and the basolateral side was filled with 1.5 mL of CAB pH 7.4. Using an EVOM epithelial voltohmmeters, TEER values across the differentiated Caco-2 cells were measured in triplicate. Only wells having a TEER value of >300 were used for the studies. The plate was preincubated in an incubator shaker for 60 min at 65 rpm along with the CAB. Donor solution (2.5 mL) for the apical side was made with the compound of interest (12.5 μL, 20 mM DMSO stock), luciferrin yellow (12.5 μL, 20 mM in water) and CAB pH 6 (2.475 mL). Donor solution (6 mL) for the basolateral side was made with the compound of interest (30 μL, 20 mM in DMSO), luciferin yellow (30 μL, 20 mM in water) and CAB pH 7.4 (5.970 mL). Luciferrin yellow was added as an internal standard in the donor solutions. The CAB solutions were aspirated and the experiment was initiated by filling the apical side with 0.5 mL of donor solution and the basolateral side with 1.5 mL of donor solution. 100 μL of samples were taken out at 0, 30, 60 and 120 minutes in triplicates from both the apical and basolateral sides and the volume was made up with the appropriate CAB.

Instrumentation and Data analysis—The samples were analyzed using Shimadzu LC-10AD HPLC using a Phenomenex Gemini 5 μm C18 (250 × 4.6 mm) column at a flow rate of 1 mL/ min. Mobile phase A was 20 mM TEAB buffer (pH 7.5) and mobile phase B was acetonitrile. P_{app} A-B and P_{app} B-A, and efflux ratio were calculated based on the cumulative sampling. The P_{app} values were calculated using equation (2):

$$P_{\text{app}}=(\frac{dQ}{dt})(1/(ACo) \quad (2)$$

where $(\frac{dQ}{dt})$ is the steady state flux, A is the surface area of the filter (cm^2) and C_0 is the initial concentration in the donor chamber.

Microsomal Stability Studies

Rat, mouse, and pooled human liver microsomes (BD Biosciences, San Jose, CA) (0.5 mg/mL) were incubated in 100 mM potassium phosphate buffer, pH 7.4 with 10 mM $MgCl_2$ and 1.0 μM **1** in a volume of 450 μL. This solution was preincubated for 5 min at 4 °C followed by 2 min at 37 °C. Water (50 μL, control reaction) or 10 mM NADPH (50 μL, microsomal reaction) were added and the two solutions were incubated for 60 min at 37 °C. After 60 min, 100 μL from each reaction was added to 200 μL acetonitrile; the resulting suspension was vortexed, centrifuged (14,000*g*, 5 min) to remove precipitated protein, and the supernatant was analyzed via LC-MS/MS as described above.

Glucuronidation Studies

1 was incubated with human and rat liver microsomes in the presence of uridine 5'-diphosphoglucuronic acid (UDPGA) under standard glucuronidation condition. Mycophenolic Acid (MPA), which is known to be rapidly metabolized by glucuronidation, was used as a positive control. Under these conditions, MPA was 85% glucuronidated by human liver microsomes at 60 min, but no glucuronide species of **1** was detected. In rat liver microsomes, glucuronidation was slower even for MPA and only 30% was glucuronidated at 60 min. Once again, glucuronidation of **1** was not detected. This confirms **1** is not a substrate for UDP-gluguronosyl transferase (UDPGT) in both human and rat liver microsomes.

Reactions were set up in duplicate in 200 μl volumes (final concentration in parenthesis). A mixture of 5 μL 20 mg protein/mL human liver microsomes (Sigma Aldrich) (0.5 mg/mL), 80 μL 0.25 M Trizma buffer pH 7.4 (0.1 M), 73 μL H_2O, 10 μL 100 mM $MgCl_2$ (5 mM), and 10 μL 0.25 mg/ml alamethicin (50 μg/mg) was prepared in each vial and incubated on ice for 30 min. 10 Ll 100 mM Saccharolactone (5 mM), and 2 μL of 60 mM MPA (600 μM) or 2 μL of 10 mM **1** (100 μM) were added to corresponding vial. The vials were pre-incubated in a 37 °C water bath for 3 min and 10 μL 60 mM UDPGA (3 mM) was added. For thermal breakdown control (lacking UDPGA), 10 μL H_2O was added. The vials were incubated for 60 min in a 37 °C water bath. The reactions were quenched at 0, 5, 15, 30, and 60 minutes by adding 200 μL crash solution (for MPA incubations: ice cold methanol with 10 μM IS; for **1** incubations: 10% TCA with 10 μM IS) to each vial. Compound **9** was used as the internal standard (IS), which has significantly different retention time compared to **1**. The vials were mixed by vortex, kept on ice for 5 min and centrifuged at 13,000 × g for 5 min. Supernatants were analyzed on LC-MS by monitoring the disappearance of **1** or MPA and the corresponding appearance of the glucuronide products at MW + 176. LC-MS was performed on an Agilent 1100 series LC-MSD trap instrument. Reverse phase LC was performed on a Zorbax SB-C18 (0.5 × 150 mm, 5 micron) column with a flow rate of 15 μL/min. The eluents and elution were as follows. Mobile phase A: 0.1% aqueous formic acid, mobile phase B: 0.1% formic acid in acetonitrile. Initial conditions were 5% B from 0 to 0.5 min, after which the %B was increased to 30% from 0.5 to 10 min, after which 30% to 95% B from 10 to 13 min. The column was washed with 95% B for 2 min, returned to 5% over 1 min, and allowed to re-equilibrate for 4 min in 5% B to provide a total run time of 20 min. The flow rate was 0.5 mL/min and the column oven was maintained at 40 °C. The injection volume was 5 μL. The MS was performed on positive ion mode using ESI.

Cell Cytotoxicity Assay

Human liver cells (HepG2, ATCC) cells were maintained in Eagle's minimum essential medium (EMEM) supplemented with 10% fetal bovine serum (FBS), 100 U/mL penicillin, and 100 μg/mL streptomycin. All reactions were performed in triplicate. Compounds (**1, 2, 4, 5, 8**, and **9**) were prepared as 20 mM stock solutions in DMSO. For the highest test concentration, 2 μL of the stock solution, 98 μL of EMEM and 100 μL of HepG2 cells in EMEM ((2.5–5.0) × 10^4 cells per well) were plated in 96-well plates, yielding a final volume of 200 μL and compound concentration of 200 μM. A serial dilution to provide final compound concentration of 100, 50, 20, 10, 5, 2, 1 μM were also prepared. Control wells contained either 1% DMSO (negative control) or 1% triton X-100 (positive control). The plate was incubated for 48 h at 37 °C in a 5% CO_2/95% air humidified atmosphere. The EMEM media was aspirated and 100 μL serum-free, phenol red free DMEM was added to each well. Measurement of cell viability was carried out using a modified method of Mosmann based on 3-(4,5-dimethylthiazol-2-yl)-2,5-diphenyltetrazolium bromide (MTT). The MTT solution was prepared fresh at 5 mg/mL in DI water. MTT solution (10 μL) was added to each well, and the plate was incubated as described above for 3 h. The MTT solution was removed, and the formazan crystals were solubilized with 200 μL of 2 N KOH. The plate was read on a M5e spectrophotometer (Molecular Devices) at 570 nm for formazan and 650 nm for background subtraction. Cell viability was estimated as the percentage absorbance of sample relative to the DMSO control. Percent cell viability was plotted against test concentration to determine CC_{50}.

Supplementary Material

Refer to Web version on PubMed Central for supplementary material.

ACKNOWLEDGMENTS

This work was supported by a grant from the National Institutes of Health Grant (RO1 AI070219 to CCA) and the Intramural Research Program of the NIAID, NIH (CEB). We thank Anja Meissner for performing the Caco-2 studies and Dr. Youlin Xia from NMR center of University of Minnesota for NMR spectroscopic analysis. Mass spectrometric analysis was carried out in the Analytical Biochemistry Shared Resource of the Masonic Cancer Center, University of Minnesota, funded in part by Cancer Center Support Grant CA-77598.

ABBREVIATIONS USED

ADME	absorption distribution metabolism excretion
appK_i	apparent inhibition constant
AUC	area under the curve
Boc	*tert*-butoxycarbonyl
C_{max}	maximum serum concentration following an oral dose
Cbz	benzyloxycarbonyl
CDI	carbonyl diimidazole
CL	clearance

DMA	dimethylacetamide
DMF	dimethylformamide
F	bioavailability
HPLC	high performance liquid chromatography
INH	isoniazid
i.v.	intravenous
MDR-TB	multidrug-resistant tuberculosis
XDR-TB	extensively drug-resistant tuberculosis
MIC	minimum inhibitory concentration
Mtb	*Mycobacterium tuberculosis*
MW	molecular weight
NHS	*N*-hydroxysuccinimide
NRPS-PKS	nonribosomal peptide synthetase–polyketide synthase
PK	pharmacokinetic
p.o.	oral
Sal-AMS	5′-*O*-[*N*-(salicyl)sulfamoyl]adenosine
SAR	structure–activity relationship
$t_{1/2}$	terminal elimination half-life following an oral dose
TB	tuberculosis
TBS	*tert*-butyldimethylsilyl
TFA	trifluoroacetic acid

REFERENCES AND NOTES

1. WHO. Global Tuberculosis Report. 2014
2. Homolka S, Niemann S, Russell DG, Rohde KH. Functional genetic diversity among *Mycobacterium tuberculosis* complex clinical isolates: delineation of conserved core and lineage-specific transcriptomes during intracellular survival. PLoS Pathog. 2010; 6:e1000988. [PubMed: 20628579]
3. Mitchison DA. Role of individual drugs in the chemotherapy of tuberculosis. Int. J. Tuberc. Lung Dis. 2000; 4:796–806. [PubMed: 10985648]
4. Jacobson KR, Tierney DB, Jeon CY, Mitnick CD, Murray MB. Treatment outcomes among patients with extensively drug-resistant tuberculosis: systematic review and meta-analysis. Clin. Infect. Dis. 2010; 51:6–14. [PubMed: 20504231]
5. Kakkar AK, Dahiya N. Bedaquiline for the treatment of resistant tuberculosis: promises and pitfalls. Tuberculosis. 2014; 94:357–362. [PubMed: 24841672]
6. Ryan NJ, Lo JH. Delamanid: first global approval. Drugs. 2014; 74:1041–1045. [PubMed: 24923253]

7. Trousseau, A. True and False Chlorosis. In: Lindsay, Blakiston; Cormack, Sir John, editors. Lectures on Clinical Medicine. 3rd Ed.. Vol. 2. London: New Sydenham Society, 1872; 1868. p. 737-751.
8. Schaible UE, Kaufmann SH. Iron and microbial infection. Nat. Rev. Microbiol. 2004; 2:946–953. [PubMed: 15550940]
9. Ratledge C. Iron, mycobacteria and tuberculosis. Tuberculosis. 2004; 84:110–130. [PubMed: 14670352]
10. Miethke M, Marahiel MA. Siderophore-based iron acquisition and pathogen control. Microbiol. Mol. Biol. Rev. 2007; 71:413–451. [PubMed: 17804665]
11. Ratledge C, Dover LG. Iron metabolism in pathogenic bacteria. Annu. Rev. Microbiol. 2000; 54:881–941. [PubMed: 11018148]
12. Twort FW, Ingram GLY. A method for isolating and cultivating the *Mycobacterium enteritidis chronicae pseudotuberculosis bovis*, Jöhne, and some experiments on the preparation of a diagnostic vaccine for pseudo-tuberculosis enteritis of bovines. Proc. R. Soc. London, Ser. B. 1912; 84:517–530.
13. Snow GA. Mycobactins - iron-chelating growth factors from mycobacteria. Bacteriol. Rev. 1970; 34:99–125. [PubMed: 4918634]
14. Vergne AF, Walz AJ, Miller MJ. Iron chelators from mycobacteria (1954–1999) and potential therapeutic applications. Nat. Prod. Rep. 2000; 17:99–116. [PubMed: 10714901]
15. Sandy M, Butler A. Microbial iron acquisition: marine and terrestrial siderophores. Chem. Rev. 2009; 109:4580–4595. [PubMed: 19772347]
16. Hider RC, Kong X. Chemistry and biology of siderophores. Nat. Prod. Rep. 2010; 27:637–657. [PubMed: 20376388]
17. Quadri LE, Sello J, Keating TA, Weinreb PH, Walsh CT. Identification of a *Mycobacterium tuberculosis* gene cluster encoding the biosynthetic enzymes for assembly of the virulence-conferring siderophore mycobactin. Chem. Biol. 1998; 5:631–645. [PubMed: 9831524]
18. Chavadi SS, Stirrett KL, Edupuganti UR, Vergnolle O, Sadhanandan G, Marchiano E, Martin C, Qiu WG, Soll CE, Quadri LE. Mutational and phylogenetic analyses of the mycobacterial *mbt* gene cluster. J. Bacteriol. 2011; 193:5905–5913. [PubMed: 21873494]
19. McMahon MD, Rush JS, Thomas MG. Analyses of MbtB, MbtE, and MbtF suggest revisions to the mycobactin biosynthesis pathway in *Mycobacterium tuberculosis*. J. Bacteriol. 2012; 194:2809–2818. [PubMed: 22447909]
20. Krithika R, Marathe U, Saxena P, Ansari MZ, Mohanty D, Gokhale RS. A genetic locus required for iron acquisition in *Mycobacterium tuberculosis*. Proc. Natl. Acad. Sci. USA. 2006; 103:2069–2074. [PubMed: 16461464]
21. De Voss JJ, Rutter K, Schroeder BG, Su H, Zhu Y, Barry CE 3rd. The salicylate-derived mycobactin siderophores of *Mycobacterium tuberculosis* are essential for growth in macrophages. Proc. Natl. Acad. Sci. USA. 2000; 97:1252–1257. [PubMed: 10655517]
22. Reddy PV, Puri RV, Chauhan P, Kar R, Rohilla A, Khera A, Tyagi AK. Disruption of mycobactin biosynthesis leads to attenuation of *Mycobacterium tuberculosis* for growth and virulence. J. Infect. Dis. 2013; 208:1255–1265. [PubMed: 23788726]
23. Jones CM, Wells RM, Madduri AV, Renfrow MB, Ratledge C, Moody DB, Niederweis M. Self-poisoning of *Mycobacterium tuberculosis* by interrupting siderophore recycling. Proc. Natl. Acad. Sci. USA. 2014; 111:1945–1950. [PubMed: 24497493]
24. Xu Y, Miller MJ. Total synthesis of mycobactin analogues as potent antimycobacterial agents using a minimal protecting group strategy. J. Org. Chem. 1998; 63:4314–4322.
25. Ferreras JA, Ryu JS, Di Lello F, Tan DS, Quadri LE. Small-molecule inhibition of siderophore biosynthesis in *Mycobacterium tuberculosis* and *Yersinia pestis*. Nat. Chem. Biol. 2005; 1:29–32. [PubMed: 16407990]
26. Miller MJ, Walz AJ, Zhu H, Wu C, Moraski G, Mollmann U, Tristani EM, Crumbliss AL, Ferdig MT, Checkley L, Edwards RL, Boshoff HI. Design, synthesis, and study of a mycobactin-artemisinin conjugate that has selective and potent activity against tuberculosis and malaria. J. Am. Chem. Soc. 2011; 133:2076–2079. [PubMed: 21275374]

27. Miethke M, Bisseret P, Beckering CL, Vignard D, Eustache J, Marahiel MA. Inhibition of aryl acid adenylation domains involved in bacterial siderophore synthesis. FEBS. J. 2006; 273:409–419. [PubMed: 16403027]
28. Somu RV, Boshoff H, Qiao C, Bennett EM, Barry CE 3rd, Aldrich CC. Rationally designed nucleoside antibiotics that inhibit siderophore biosynthesis of *Mycobacterium tuberculosis*. J. Med. Chem. 2006; 49:31–34. [PubMed: 16392788]
29. Manos-Turvey A, Bulloch EM, Rutledge PJ, Baker EN, Lott JS, Payne RJ. Inhibition studies of *Mycobacterium tuberculosis* salicylate synthase (MbtI). ChemMedChem. 2010; 5:1067–1079. [PubMed: 20512795]
30. Vergnolle O, Xu H, Blanchard JS. Mechanism and regulation of mycobactin fatty acyl-AMP ligase FadD33. J. Biol. Chem. 2013; 288:28116–28125. [PubMed: 23935107]
31. Vickery CR, Kosa NM, Casavant EP, Duan S, Noel JP, Burkart MD. Structure, biochemistry, and inhibition of essential 4'-phosphopantetheinyl transferases from two species of mycobacteria. ACS Chem. Biol. 2014; 9:1939–1944. [PubMed: 24963544]
32. Somu RV, Wilson DJ, Bennett EM, Boshoff HI, Celia L, Beck BJ, Barry CE 3rd, Aldrich CC. Antitubercular nucleosides that inhibit siderophore biosynthesis: SAR of the glycosyl domain. J. Med. Chem. 2006; 49:7623–7635. [PubMed: 17181146]
33. Qiao CH, Gupte A, Boshoff HI, Wilson DJ, Bennett EM, Somu RV, Barry CE 3rd, Aldrich CC. 5'-*O*-[(*N*-Acyl)sulfamoyl]adenosines as antitubercular agents that inhibit MbtA: An adenylation enzyme required for siderophore biosynthesis of the mycobactins. J. Med. Chem. 2007; 50:6080–6094. [PubMed: 17967002]
34. Neres J, Labello NP, Somu RV, Boshoff HI, Wilson DJ, Vannada J, Chen L, Barry CE 3rd, Bennett EM, Aldrich CC. Inhibition of siderophore biosynthesis in *Mycobacterium tuberculosis* with nucleoside bisubstrate analogues: structure-activity relationships of the nucleobase domain of 5'-*O*-[*N*-(salicyl)sulfamoyl]adenosine. J. Med. Chem. 2008; 51:5349–5370. [PubMed: 18690677]
35. Labello NP, Bennett EM, Ferguson DM, Aldrich CC. Quantitative three dimensional structure linear interaction energy model of 5'-*O*-[*N*-(salicyl)sulfamoyl]adenosine and the aryl acid adenylating enzyme MbtA. J. Med. Chem. 2008; 51:7154–7160. [PubMed: 18959400]
36. Neres J, Wilson DJ, Celia L, Beck BJ, Aldrich CC. Aryl acid adenylating enzymes involved in siderophore biosynthesis: fluorescence polarization assay, ligand specificity, and discovery of non-nucleoside inhibitors via high-throughput screening. Biochemistry. 2008; 47:11735–11749. [PubMed: 18928302]
37. Lun S, Guo H, Adamson J, Cisar JS, Davis TD, Chavadi SS, Warren JD, Quadri LE, Tan DS, Bishai WR. Pharmacokinetic and in vivo efficacy studies of the mycobactin biosynthesis inhibitor salicyl-AMS in mice. Antimicrob. Agents Chemother. 2013; 57:5138–5140. [PubMed: 23856770]
38. Beaumont K, Webster R, Gardner I, Dack K. Design of ester prodrugs to enhance oral absorption of poorly permeable compounds: challenges to the discovery scientist. Curr. Drug. Metab. 2003; 4:461–485. [PubMed: 14683475]
39. Ikeuchi H, Meyer ME, Ding Y, Hiratake J, Richards NG. A critical electrostatic interaction mediates inhibitor recognition by human asparagine synthetase. Bioorg. Med. Chem. 2009; 17:6641–6650. [PubMed: 19683931]
40. Kurokawa T, Kim M, Du Bois J. Synthesis of 1,3-diamines through rhodium-catalyzed C-H insertion. Angew. Chem. Int. Ed. 2009; 48:2777–2779.
41. Mitsunobu O. The use of diethyl azodicarboxylate and triphenylphosphine in synthesis and transformation of natural products. Synthesis. 1981:1–28.
42. Vannada J, Bennett EM, Wilson DJ, Boshoff HI, Barry CE 3rd, Aldrich CC. Design, synthesis, and biological evaluation of beta-ketosulfonamide adenylation inhibitors as potential antitubercular agents. Org. Lett. 2006; 8:4707–4710. [PubMed: 17020283]
43. Aldrich C, Somu RV. Antibacterial Agents. 2011 Aug 2. U.S. Patent 7,989,430.
44. Lu X, Zhang H, Tonge PJ, Tan DS. Mechanism-based inhibitors of MenE, an acyl-CoA synthetase involved in bacterial menaquinone biosynthesis. Bioorg. Med. Chem. Lett. 2008; 18:5963–5966. [PubMed: 18762421]
45. Hagmann WK. The many roles for fluorine in medicinal chemistry. J. Med. Chem. 2008; 51:4359–4369. [PubMed: 18570365]

46. Robins MJ, Uznanski B. Nucleic-acid related compounds. 33. Conversions of adenosine and guanosine to 2,6-dichloro, 2-amino-6-chloro, and derived purine nucleosides. Can. J. Chem. 1981; 59:2601–2607.
47. Matsuda A, Shinozaki M, Yamaguchi T, Homma H, Nomoto R, Miyasaka T, Watanabe Y, Abiru T. Nucleosides and nucleotides. 103. 2-Alkynyladenosines – A novel class of selective adenosine-A2 receptor agonists with potent antihypertensive effects. J. Med. Chem. 1992; 35:241–252. [PubMed: 1732541]
48. Lakshman MK, Hilmer JH, Martin JQ, Keeler JC, Dinh YQ, Ngassa FN, Russon LM. Palladium catalysis for the synthesis of hydrophobic C-6 and C-2 aryl 2'-deoxynucleosides. Comparison of C-C versus C-N bond formation as well as C-6 versus C-2 reactivity. J. Am. Chem. Soc. 2001; 123:7779–7787. [PubMed: 11493051]
49. Takai H, Obase H, Nakamizo N, Teranishi M, Kubo K, Shuto K, Hashimoto T. Synthesis and pharmacological evaluation of piperidine derivatives with various heterocyclic rings at the 4-position. Chem. Pharm. Bull. 1985; 33:1104–1115. [PubMed: 4028293]
50. Wnuk SF, Companioni DR, Neschadimenko V, Robins MJ. The beta-fluorine effect. Electronic versus steric effects in radical deoxygenations of fluorine-containing pentofuranose nucleosides. J. Org. Chem. 2002; 67:8794–8797. [PubMed: 12467391]
51. Liu F, Austin DJ. A general synthesis of 5'-azido-5'-deoxy-2'.3'-*O*-isopropylidene nucleosides. J. Org. Chem. 2001; 66:8643–8645. [PubMed: 11735550]
52. Belanger PM, Lalande M, Dore FM, Labrecque G. Temporal variations in the pharmacokinetics of isoniazid and *N*-acetylisoniazid in rats. Drug. Metab. Dispos. 1989; 17:91–97. [PubMed: 2566477]
53. Baldan HM, De Rosa HJ, Brunetti IL, Ximenes VF, Machado RGP. The effect of rifampicin and pyrazinamide on isoniazid pharmacokinetics in rats. Biopharm. Drug Dispos. 2007; 28:409–413. [PubMed: 17828712]
54. Ferraris D, Duvall B, Delahanty G, Mistry B, Alt J, Rojas C, Rowbottom C, Sanders K, Schuck E, Huang KC, Redkar S, Slusher BB, Tsukamoto T. Design, synthesis, and pharmacological evaluation of fluorinated tetrahydrouridine derivatives as inhibitors of cytidine deaminase. J. Med. Chem. 2014; 57:2582–2588. [PubMed: 24520856]
55. Alex A, Millan DS, Perez M, Wakenhut F, Whitlock GA. Intramolecular hydrogen bonding to improve membrane permeability and absorption in beyond rule of five chemical space. Med. Chem. Commun. 2011:669–674.
56. O'Shea R, Moser HE. Physicochemical properties of antibacterial compounds: implications for drug discovery. J. Med. Chem. 2008; 51:2871–2878. [PubMed: 18260614]
57. Duckworth BP, Nelson KM, Aldrich CC. Adenylating enzymes in *Mycobacterium tuberculosis* as drug targets. Curr. Top. Med. Chem. 2012; 12:766–796. [PubMed: 22283817]
58. Schmelz S, Naismith JH. Adenylate-forming enzymes. Curr. Opin. Struct. Biol. 2009; 19:666–671. [PubMed: 19836944]
59. Kalinda AS, Bockman MR, Petrelli R, de la Mora T, Shi C, Tawari D, Schnappinger D, Finzel BC, Aldrich CC. Targeting *Mycobacterium tuberculosis* biotin protein ligase (MtBPL). Synthesis and evaluation of nucleoside-based bisubstrate adenylation inhibitors. unpublished results.
60. Copeland, RA. Evaluation of Enzyme Inhibitors in Drug Discovery. Hoboken, NJ: Wiley; 2005.
61. Hubatsch I, Ragnarsson EG, Artursson P. Determination of drug permeability and prediction of drug absorption in Caco-2 monolayers. Nat. Protoc. 2007; 2:2111–2119. [PubMed: 17853866]

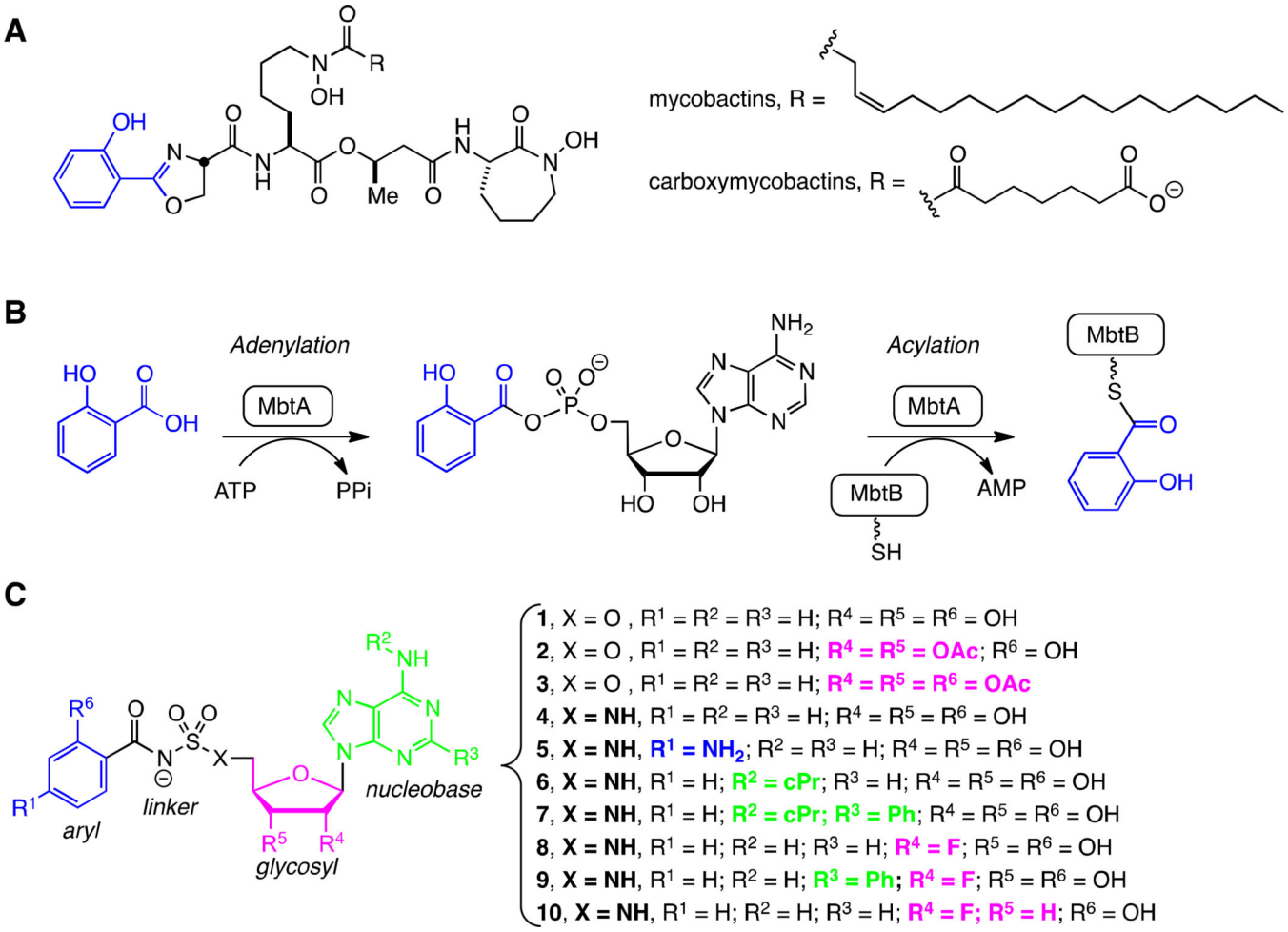

Figure 1.

Mycobactins, biosynthesis, and inhibitors. **A**. Structures of the lipid soluble mycobactins and water soluble mycobactins (refered to as carboxymycobactins) produced by *Mtb*. The mycobactins and carboxymycobactins are synthesized as a suite of compounds that differ in the chain length of the lipid tail on the central lysine residue. The most abundant chain length is depicted. **B**. Biosynthesis of all mycobactins is initiated with the ATP-dependent activation of salicylic acid by MbtA to form an intermediate acyl-adenylate. In a second half-reaction, MbtA ligates salicylic acid onto the N-terminal aryl acid carrier protein domain of MbtB. MbtB, in combination with MbtE, MbtC, MbtD, and MbtF (not shown), sequentially builds the mycobactin peptidic core scaffold. **C**. 5′-*O*-[*N*-(salicyl)sulfamoyl]adenosine (**1**) was the first described inhibitor of MbtA and is considered a bisubstrate inhibitor that mimics the intermediate acyl-adenylate. This modular inhibitor scaffold contains aryl (blue), linker (black), glycosyl (pink), and nucleobase (green) domains. Prior SAR studies have examined the importance of each atom of this scaffold and provided a comprehensive understanding of the structure-activity relationships (SAR) that govern enzyme inhibition and whole-cell activity. This information has been used to design prodrugs **2**–**3** and analogs **4**–**10** in order to explore the SAR that governs pharmacokinetic behavior.

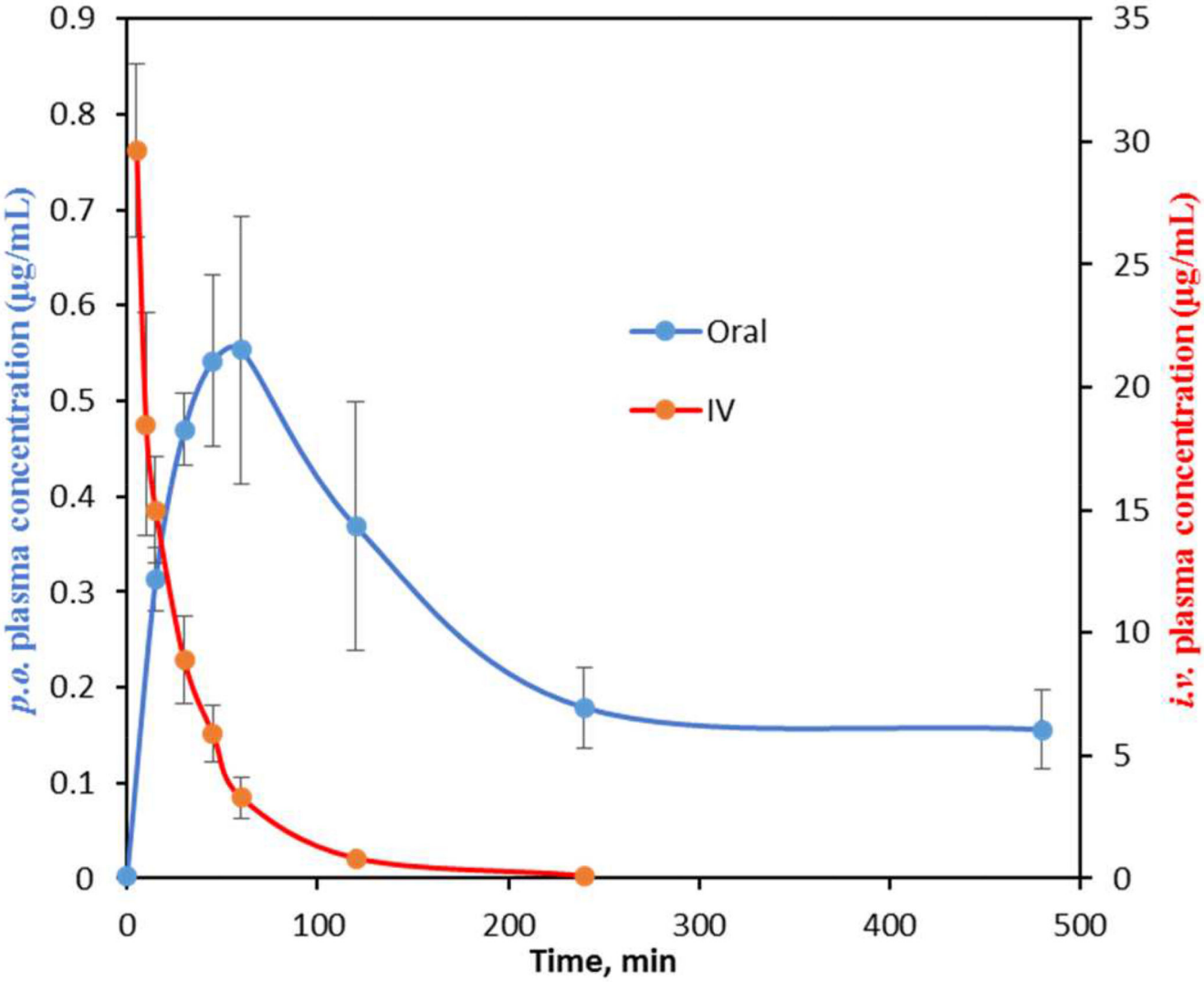

Figure 2.

Mean plasma concentration *vs*. time curves of single dosage of compound **10** in 3 rats by both *p.o*. and *i.v*. administration. Error bars represent the standard deviation of the mean (n=3).

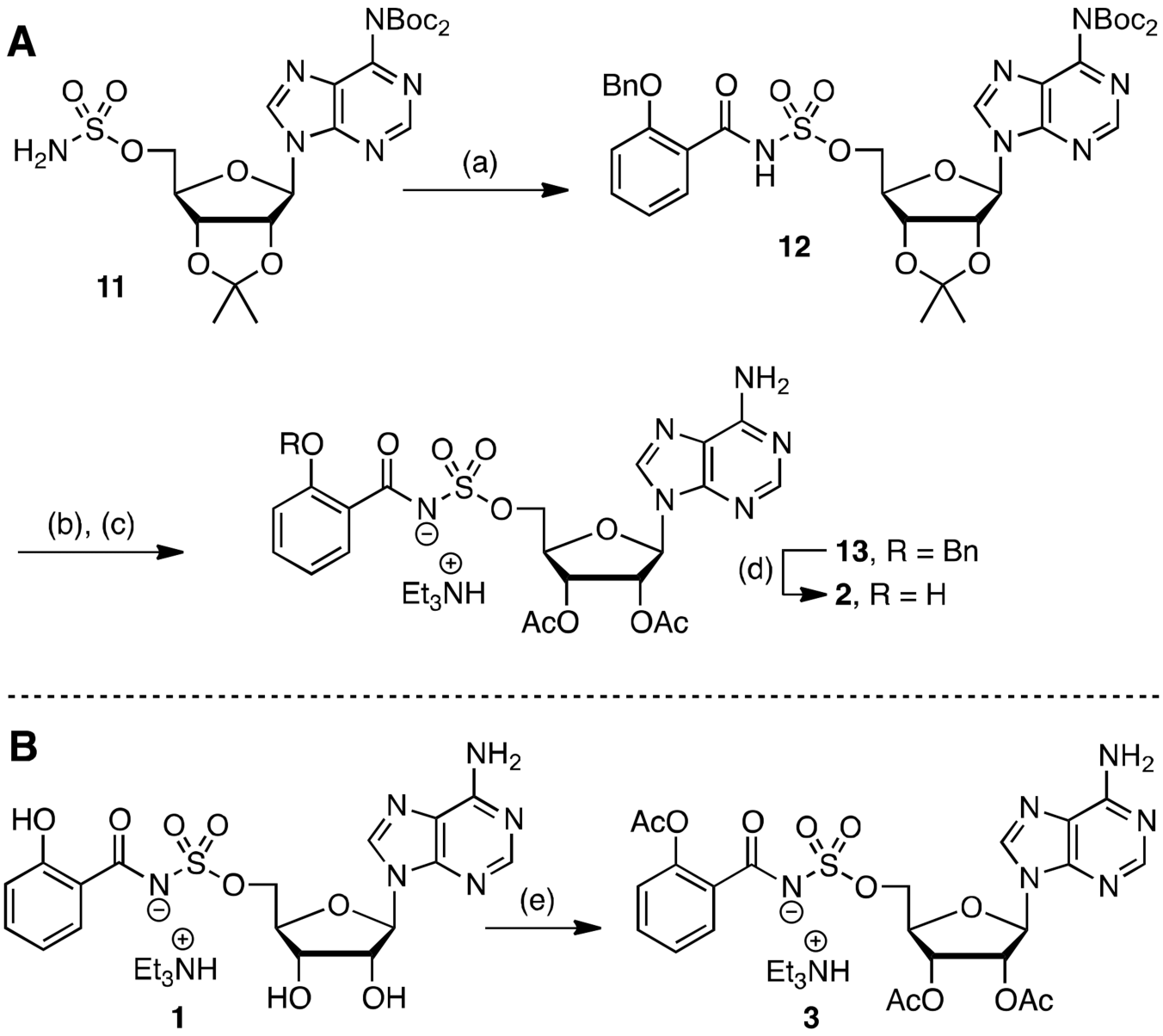

Scheme 1. a. Synthesis of prodrugs 2 and 3

[a]Reaction conditions: (a) *N*-hydroxysuccinimidyl 2-benzyloxybenzoate, Cs_2CO_3, DMF, 0 °C to rt, 21 h, 62%; (b) 80% aqueous TFA, 0 °C to rt, 4 h; (c) Ac_2O, pyridine, DMF, rt, 16 h, 63% (2 steps); (d) H_2, Pd/C, MeOH, rt, 2 h, 42%; (e) Ac_2O, pyridine, DMF, rt, 20 h, 46%.

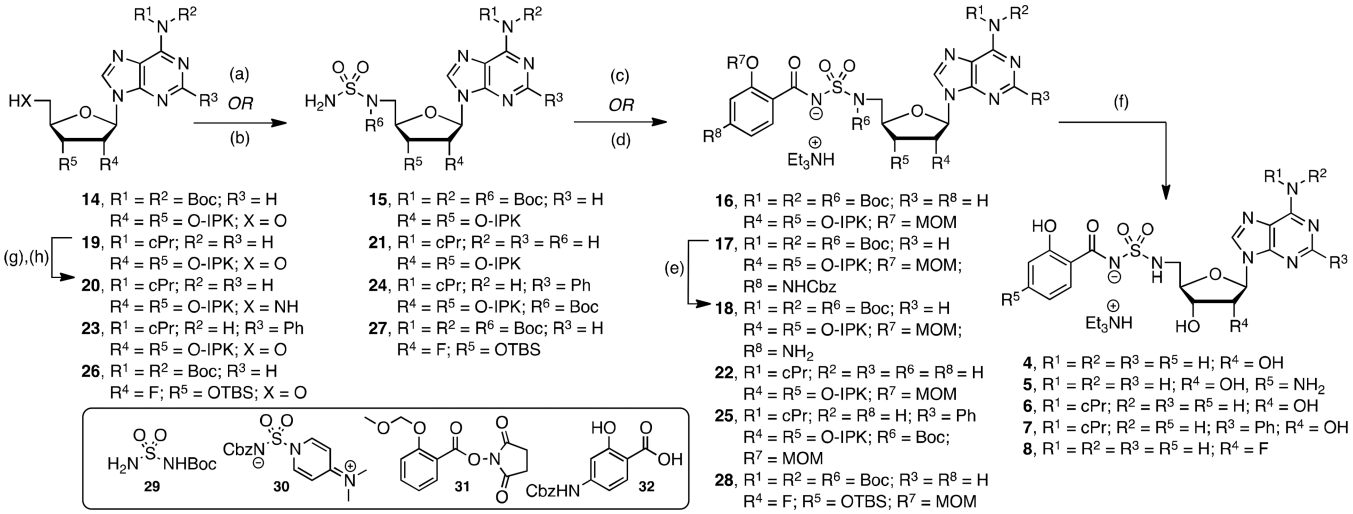

Scheme 2. a. Synthesis of 4–8

[a]Reaction conditions: (a) **29**, PPh_3, DIAD, THF, 0 °C to rt, 16 h, **15**=96%, **24**=91%, **27**=89%; (b) *i)***30**, CH_2Cl_2, rt, 14 h; *ii)* then H_2, Pd/C, MeOH–THF, rt, 22 h, **21**=62%; (c) **31**, Cs_2CO_3, DMF, 0 °C to rt, 16 h, **16**=60%, **22**=43%; (d) *i)***32**, CDI, THF, 60 °C, 2 h; *ii)* then **15**, Cs_2CO_3, THF, rt, 16 h, **17**=55%; (e) H_2, Pd/C, MeOH, rt, 2 h; (f) 80% aqueous TFA, 0 °C to rt, 4 h, **4**=65%, **5**=34% (2 steps from **17**), **6**=61%, **7**=18% (2 steps from **24**), **8**=38 % (2 steps from **27**); (g) DPPA, NaN_3, 15-crown-5, THF, 0 °C to rt, 4.5 h; (h) H_2, Pd/C, MeOH, rt, **20**=44%, (2 steps from **19**). Nonstandard abbreviations: IPK = isopropylidene ketal.

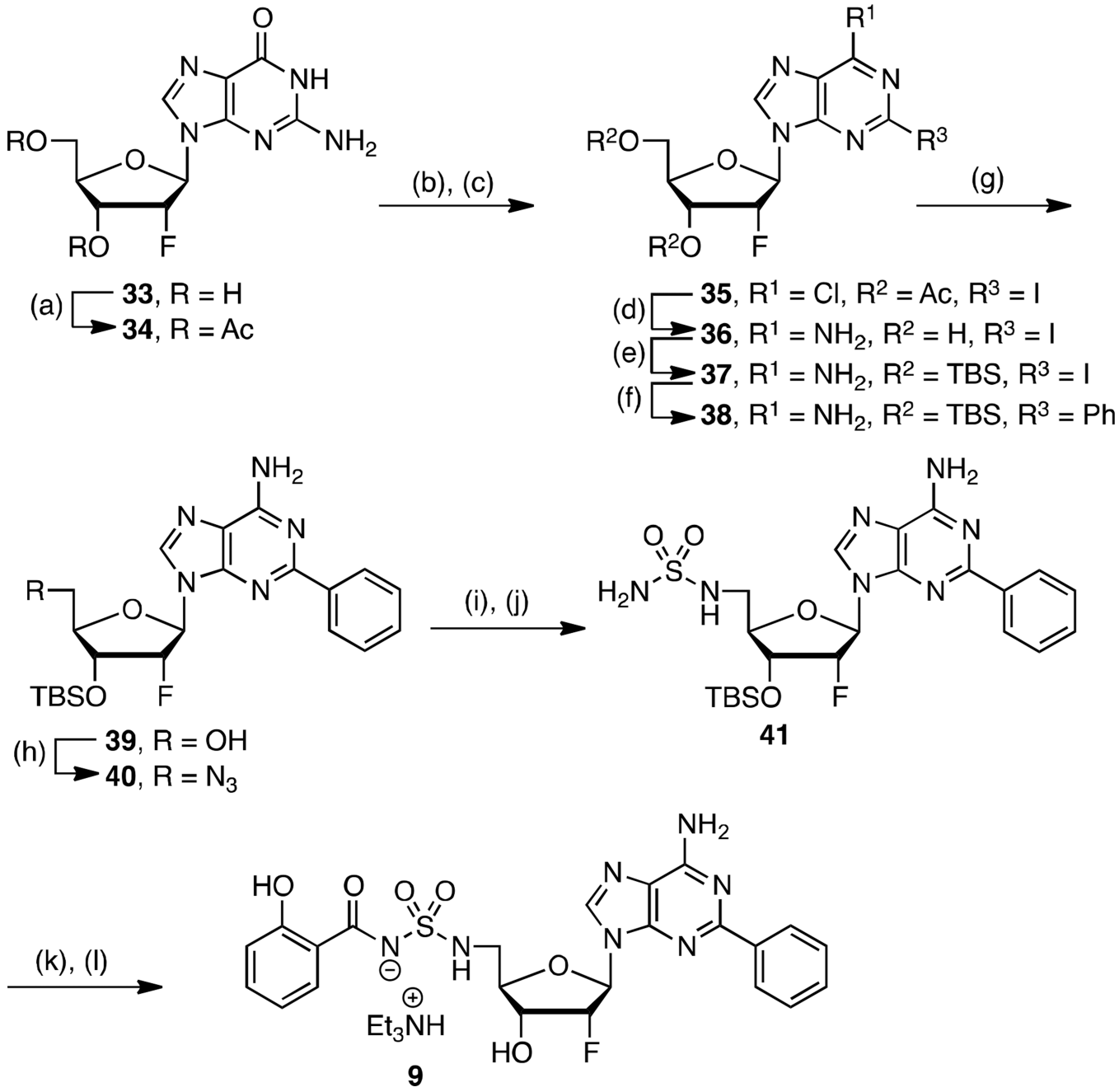

Scheme 3. a. Synthesis of 9

[a]Reaction conditions: (a) Ac_2O, pyridine, DMF, rt, 12 h, 79%; (b) $POCl_3$, DMA, Et_4NCl, reflux, 20 min, 86%; (c) CH_2I_2, I_2, isoamylnitrite, 80 °C, 1 h, 95%; (d) NH_3, MeOH, 70 °C, 24 h, 56%; (e) TBSCl, imidazole, DMAP, DMF, rt, 24 h, 97%; (f) $Pd(OAc)_2$, CyJohnPhos, K_3PO_4, $Ph(BOH)_2$, 100 °C, 12 h, 67%; (g) AcOH–THF–H_2O (9:1:1), THF, 23 °C, 24 h, 70%; (h) DPPA, DBU, NaN_3, 15-crown-5, 24 h, 85%; (i) Pd/C, MeOH, rt, 1 h; (j) $NH_2SO_2NH_2$, dioxane, 90 °C, 3 h, 87% (2 steps); (k) **31**, Cs_2CO_3, DMF, 0 °C to rt, 16 h; (l) 80% aq TFA, 0 °C, 3 h, 45% (2 steps from **41**). Nonstandard abbreviations: CyJohnPhos = (2-biphenyl)dicyclohexylphosphine.

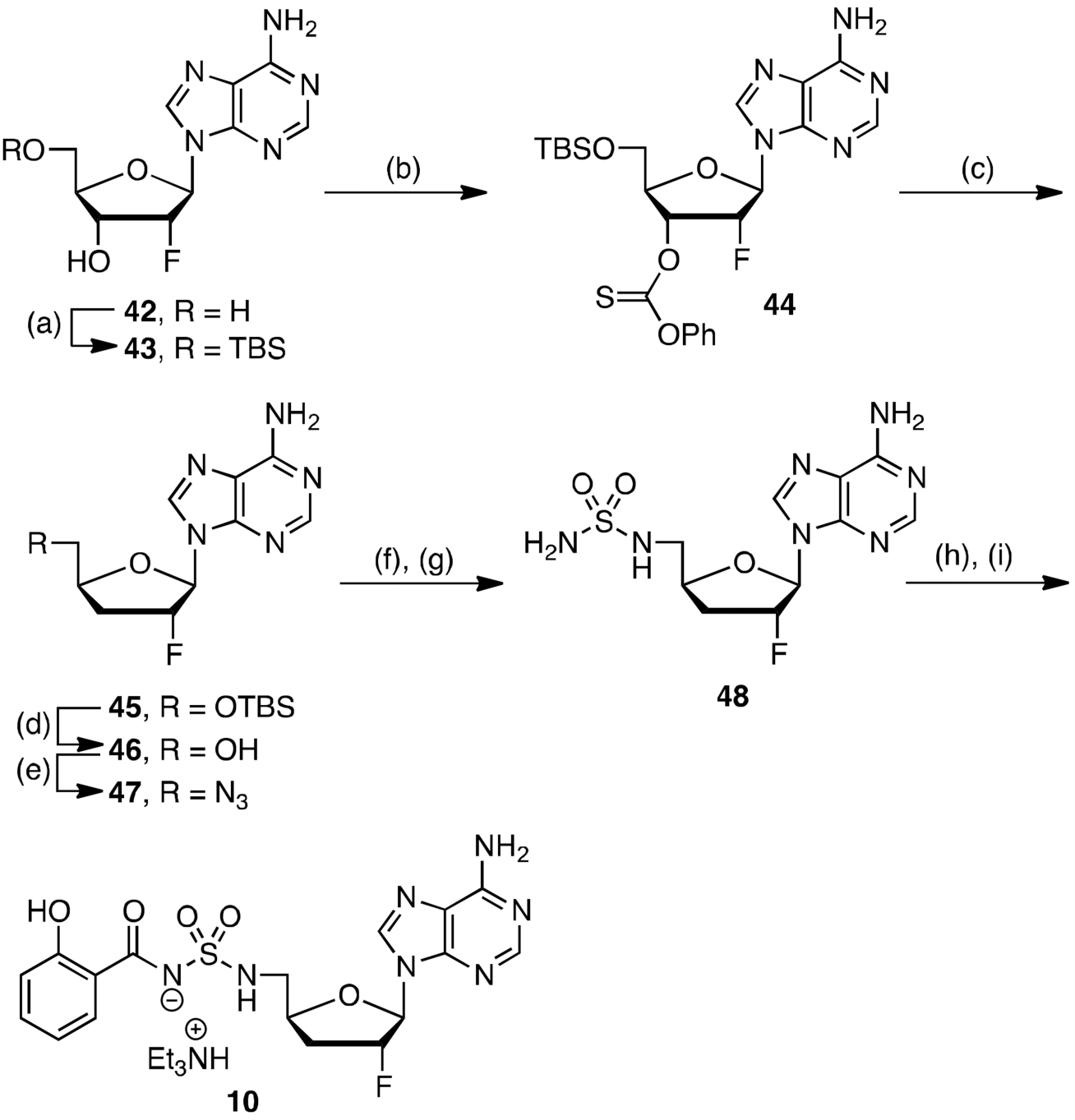

Scheme 4. a. Synthesis of 10

[a]Reaction conditions: (a) TBSCl, imidazole, DMF, 23 °C, 7 h, 90%; (b) *O*-phenyl chlorothionoformate, DMAP, MeCN, 23 °C, 1 h, 82%; (c) Bu_3SnH, AIBN, toluene, 85 °C, 3 h,79%; (d) TFA, MeOH, 0 °C, 12 h, 92%; (e) *i)* DPPA, DBU, dioxane, 23 °C, 12 h; *ii)* NaN_3, 15-crown-5, dioxane, 90 °C, 12 h, 66%; (f) Pd/C, MeOH, 23 °C, 1 h; (g) $NH_2SO_2NH_2$, dioxane, 90 °C, 3 h, 60% (2 steps); (h) **31**, Cs_2CO_3, DMF, 0 °C to rt, 16 h; (i) 80% aq TFA, 0 °C, 1 h, 34% (2 steps from **48**).

Table 1

Enzyme inhibition and antimycobacterial activity of **1** analogs.

Compound	appK_i, (nM)[a]	MIC, μM (μg/mL)[b]	MIC/appK_i[c]	CC_{50} (μM)[d]
1	6.6 ± 1.5	0.39 (0.20)	59	>200
4	3.7 ± 0.6	0.19 (0.11)	51	>200
5	8.9 ± 0.7	3.125 (1.81)	351	>200
6	1.5 ± 0.2	0.098 (0.06)	65	–
7	0.76 ± 0.40	6.25 (4.27)	8224	–
8	1.7 ± 0.1	0.19 (0.11)	112	>200
9	1.6 ± 0.1	1.56 (1.0)	975	>200
10	3.0 ± 0.2	0.78 (0.43)	260	–

[a] Assay performed with 7 nM MbtA, 10 mM ATP, 250 μM salicylic acid, 1 mM PPi.

[b] Grown in glycerol-alanine salts (GAS) medium without ferric ammonium citrate at pH 6.6.

[c] both in units of μM.

[d] Cell cytotoxicity of HepG2 cells resulting in loss of 50% viability.

Table 2

Pharmacokinetic parameters of **1** analogs.

Compound	*i.v.* PK parameters[a]			*p.o.* PK parameters[b]		
	$AUC_{0\text{-}inf}$ ($min \cdot \mu g \cdot mL^{-1}$)	CL ($mL \cdot min^{-1} \cdot kg^{-1}$)	$t_{1/2}$ (min)	C_{max} ($\mu g \cdot mL^{-1}$)	$AUC_{0\text{-}inf}$ ($\mu g \cdot min \cdot mL^{-1}$)	F (%)
1	519 ± 115	4.9 ± 0.9	11 ± 2	0.4 ± 0.2	66 ± 41	1.3 ± 0.7
2	nd	nd	nd	<LD	<LD	na
3	nd	nd	nd	0.03 ± 0.01	2.9 ± 0.8	na
4	304 ± 60	8.4 ± 1.9	10.6 ± 0.7	0.70 ± 0.07	99.8 ± 13.6	3.5 ± 0.2
5	63 ± 47	46.3 ± 4.5	10.6 ± 2.1	0.09 ± 0.01	16.8 ± 4.2	3.7 ± 0.3
6	209 ± 76	9.6 ± 0.1	15.1 ± 1.3	0.14 ± 0.01	18.1 ± 2.1	1.0 ± 0.4
7	184 ± 30	13.6 ± 2	15.5 ± 10.6	0.10 ± 0.01	4.0 ± 0.9	0.3 ± 0.1
8	1043 ± 326	2.5 ± 0.9	32.5 ± 7.4	0.46 ± 0.30	188 ± 110	1.8 ± 0.9
9	1981 ± 200	1.3 ± 0.1	121 ± 18	0.50 ± 0.16	140 ± 46	0.80 ± 0.15
10	959 ± 135	2.6 ± 0.5	62 ± 6.4	0.56 ± 0.12	198 ± 49	2.0 ± 0.08

[a] *i.v.* dose ($D_{i.v.}$) = 2.5 mg/kg.

[b] *p.o.* dose ($D_{p.o.}$) = 25 mg/kg. Values are reported as the mean ± SD. $AUC_{0\text{-}inf}$: area under the plasma concentration-time curve from time 0 to infinity, CL: clearance, $t_{1/2}$: terminal elimination half-life, C_{max}: maximum plasma concentration, F: relative oral bioavailability calculated as follows $F = 100 \times [(AUC_{p.o} \times D_{i.v.})/(AUC_{i.v.} \times D_{p.o.})]$, nd: not determined, na: not applicable, LD: below the limit of detection.

Table 3

Caco-2 permeability studies of select compounds.

Compound	P_{app}, A to B 10^{-6} cm/s	P_{app}, B to A 10^{-6} cm/s	efflux ratio
1	1.23	0.96	0.78
2	0.62	0.97	1.55
4	1.23	0.86	0.69
7	0.52	1.8	3.45
8	4.20	1.34	0.32

Table 4

Mass spectrometry ionization parameters.

Compound	Parent Ion (*m/z*)	Fragment Ion (*m/z*)	Declustering Potential (V)	Collision Energy (V)	Collision Cell Exit Potential (V)
INH	138.0	177.2	40	19	24
1	467.1	347.2	130	25	16
2	551.0	352.2	140	23	19
3	593.0	352.1	80	26	20
4	466.1	267.1	60	23	14
5	506.1	369.1	79	30	14
6	481.0	136.1	140	51	18
7	582.3	383.0	140	30	13
8	468.0	269.2	140	24	13
9	544.2	345.2	52	24	20
10	452.0	315.0	140	23	18